

Methods for Thin Nearly Flat Elastic Shells with Stretching and Bending

“Frozen Shapes: Thin Nearly Flat Elastic Shells with Stretching and Bending” problem presented by
Dr. John Abbott, Corning Inc. (June 22, 2015)

Industrial Participants

John Abbott (abbottjs@corning.com)

Les Button (buttonlj@corning.com)

Contributors

Mahdi Bandegi (mb495@njit.edu)

Aaron Bardall (arbardal@ncsu.edu)

Valeria Barra (vb82@njit.edu)

Sean Bohun (sean.bohun@uoit.ca)

Peter Buchak (p.buchak@imperial.ac.uk)

Darren Crowdy (d.crowdy@imperial.ac.uk)

Andrew deStefan (destefan@njit.edu)

Pavel Dubovski (pdubovsk@stevens.edu)

Hangjie Ji (hangjie@math.duke.edu)

Shelvean Kapita (kapita@udel.edu)

Longfei Li (lil19@rpi.edu)

Jared Little (jared.little@duke.edu)

Michael Mazzoleni (michael.mazzoleni@duke.edu)

Bob Ronkese (ronkeser@usmma.edu)

Ray Walsh (rpwalsh@sfu.ca)

Thomas Witelski (witelski@math.duke.edu)

Maxim Zyskin (zyskin@yahoo.com)

Summary Presentation given by Ray Walsh (June 26, 2015)

Summary Report compiled by Jared Little and Thomas Witelski (April 2, 2016)

1 Introduction

Many technological applications are imposing increasing tight specifications on manufacturing processes in order to construct high-precision products that are thinner, lighter, and more inexpensive. In the context of producing large video displays, there is a need to produce very thin glass sheets and identify any imperfections that can cause deviations from being perfectly flat and uniform. For large thin glass sheets, variations can be introduced due to the glass forming process (possibly yielding large out-of-plane perturbations) and subsequent thermal stresses that can generate further deflections of the sheet during cooling of the glass.

In this context, this project examined approaches for describing the steady-state deflection of large thin glass sheets [9].¹ We consider the glass as a thin, nearly planar sheet of an ideally elastic material. The aspect ratio of thickness h to the length and width dimensions L is small; a typical thickness is around 0.5 mm and a typical width is 2 m.

Due to small non-idealities during manufacturing, the sheet may end up not exactly flat. The initial “stress free” out-of-plane deflection (in the z -direction) of the hot glass sheet will be represented as $w_0(x, y)$. The ideally flat sheet has $w_0 = 0$. We are interested in the case where $|w_0/L| \ll 1$, but is it not true that $|w_0| \ll h$: indeed it is very possible for the magnitude of w_0 to be 10 to 20 times larger than h .

The cooling of the sheet may also produce non-uniformities due to ‘frozen-in’ strain due to thermal stresses [15–18]. We denote this influence by $\alpha T(x, y)$, representing the product of the thermal expansion coefficient with the deviation of the local glass temperature from the uniform ambient temperature.² It is assumed that this strain does not vary through the sheet thickness and so does not *necessarily* introduce bending type deformations.³ For a flat sheet, and

¹From material prepared by Jared Little

² $T(x, y) = T_{\text{local}}(x, y) - T_{\text{amb}}$.

³Note that αT is written as if it represents a thermal strain, but in reality it is simply some non-uniform but isotropic strain that results from a non-ideal thermal history: the density of glass is actually a function of cooling rate, so small non-uniformities in cooling may lead to small strains in the final glass sheet, even in isothermal conditions. However this strain behaves in exactly the same way that a strain field caused by non-uniform temperature would behave.

Parameter	Symbol	Value
Sheet Thickness	h	0.5-0.7 mm
Sheet Width	W	1500 mm
Sheet Length	L	2000 mm
Young's Modulus	E	70 GPa
Poisson's Ratio	ν	0.22
Coeff. of Therm. Exp.	α	$5 \times 10^{-6} \text{ K}^{-1}$

Table 1: Parameter values for system (1.1ab).

for small enough initial strains αT , the strain can only lead to “in-plane” stress; for larger initial strains, buckling instability could develop and deformations involving bending as well as in-plane deformation may occur.

Our goal is to understand how these two influence can interact. Namely,

1. Given w_0 and αT what is the simplest mathematical model that accurately describes the overall deflection, and what are efficient computational strategies for numerical solving the governing equations.
2. Given the overall deflection and measured data for αT , can w_0 be recovered?
3. Given the overall deflection and estimates for w_0 , can αT be recovered?

With the governing equations identified, the first question is called a “forward problem” involving direct evaluation of the model given all needed parameters and system data. In contrast the latter two questions are called “inverse problems.” Whether either of these inverse problems is well-posed (that is, if they can be accurately solved with low sensitivity to noise in the given data) is not clear. A further related question would be if the stress-free and stress-induced components of the deflection could be separated out from just the overall deflection and some general assumptions about the forms of each contribution.

While these questions about inverse problems are the ultimate long-term goals in this class of manufacturing problems, for the workshop, primary attention was focused studying the forward problem. In particular, using the large separation in lengthscales between the length and thickness of the sheet, asymptotics can be used to reduce the full governing equations of solid mechanics down to more tractable forms. For transverse deflections of a nominally flat thin sheet (with $w_0 \equiv 0$), called a “plate” there are well-known von Karman plate models [10,13]. Versions of such plate models incorporating in-plane thermal stresses are available in several references [19, Eq. 18.31]. Conversely, in the absence of thermal stresses, the governing equations for equilibrium configurations of deformed sheets (with $w_0 \neq 0$), called shells, are available from other sources [6, Chapter 7]. In particular, one of the original questions posed in the project is whether the straightforward expected combination of these respective governing models yields a consistent model:

$$-\frac{1}{Eh} \nabla^4 \varphi = \left(\frac{\partial^2 w_0}{\partial x^2} \frac{\partial^2 w}{\partial y^2} - 2 \frac{\partial^2 w_0}{\partial x \partial y} \frac{\partial^2 w}{\partial x \partial y} + \frac{\partial^2 w_0}{\partial y^2} \frac{\partial^2 w}{\partial x^2} \right) + \left(\frac{\partial^2 w}{\partial x^2} \frac{\partial^2 w}{\partial y^2} - \left(\frac{\partial^2 w}{\partial x \partial y} \right)^2 \right) + \nabla^2 (\alpha T) \quad (1.1a)$$

$$D \nabla^4 w = \left(\frac{\partial^2 w_0}{\partial x^2} \frac{\partial^2 \varphi}{\partial y^2} - 2 \frac{\partial^2 w_0}{\partial x \partial y} \frac{\partial^2 \varphi}{\partial x \partial y} + \frac{\partial^2 w_0}{\partial y^2} \frac{\partial^2 \varphi}{\partial x^2} \right) + \left(\frac{\partial^2 w}{\partial x^2} \frac{\partial^2 \varphi}{\partial y^2} - 2 \frac{\partial^2 w}{\partial x \partial y} \frac{\partial^2 \varphi}{\partial x \partial y} + \frac{\partial^2 w}{\partial y^2} \frac{\partial^2 \varphi}{\partial x^2} \right) + P_{\text{ext}} \quad (1.1b)$$

where w is the transverse deflection, φ is the Airy stress function, h is the thickness of the sheet, E is the Young's Modulus, α is the coefficient of thermal expansion, T is temperature, p is pressure due to any applied load, and

$$D = \frac{Eh^3}{12(1-\nu^2)} \quad (1.2)$$

is the plate's bending stiffness where ν is the Poisson's ratio. In this case, we are not primarily concerned with external pressure or applied loads and take $P_{\text{ext}} = 0$. Table 1 gives a summary of the parameters with values appropriate for the rectangular glass sheets.

To give a complete problem statement for the coupled elliptic PDEs (1.1ab), boundary conditions are needed. To focus attention on the spatial structure of deflections due to internal stresses, free boundary conditions are applied to all edges of the glass sheets, on the deflection [7,8],

$$\frac{\partial^2 w}{\partial n^2} + \nu \frac{\partial^2 w}{\partial s^2} \Big|_{\partial\Omega} = 0, \quad \frac{\partial}{\partial n} (\nabla^2 w) + (1-\nu) \frac{\partial}{\partial s} \left(\frac{\partial^2 w}{\partial n \partial s} \right) \Big|_{\partial\Omega} = 0, \quad (1.3a)$$

where n is the coordinate normal to a straight segment of the boundary and s is the coordinate along the boundary, along with conditions on the normal stress in terms of the Airy stress function,

$$\left. \frac{\partial^2 \varphi}{\partial n^2} \right|_{\partial\Omega} = 0, \quad \left. \frac{\partial^2 \varphi}{\partial n \partial s} \right|_{\partial\Omega} = 0, \quad (1.3b)$$

where the components of the stress are given by $\sigma_x = \partial^2 \varphi / \partial y^2$, $\sigma_y = \partial^2 \varphi / \partial x^2$, and $\tau_{xy} = -\partial^2 \varphi / \partial x \partial y$. These boundary conditions also generally correspond to the typical situation in handling the glass sheets, which might be suspended from one edge or pinned at a small number of interior points.

A fundamental question is that while we have formally written equations (1.1ab) to incorporate thermal stresses in a shell model, this system has not been derived starting from first principles (e.g. kinematics of strain in a curved shell *including* the initial strain); instead they are assumed appropriate because they combine terms found in different sections of various texts, where loaded shells and thermoelastic problems are treated separately. In fact, equation (1.1a) appears to introduce a puzzle: it does not seem to be physically consistent with an apparently trivial special case of uniform initial strain. Imagine that the initial shape is a shallow “spherical cap” with radius R . The shell is then heated and achieves an increased but spatially uniform temperature. Under these conditions, the overall sheet simply grows in size in all dimensions by the same fractional amount αT ; the radius of curvature increases from R to some new value $R' > R$. We assume all boundaries are free, and there is no internal spatial variation in the thermal strain, so the “expanded” state is stress free. However, equation (1.1a) has a *finite* right-hand side, because of the change in Gaussian curvature of the surface, while there is no contribution from the spatially uniform initial strain field since it appears inside the Laplacian. The equation thus predicts finite stress, that is a non-trivial stress potential φ , for a situation which should be stress free. Whether this model has something missing (or included erroneously) in the governing equations needs to be examined closely.

The following sections outline work carried out by the group during the MPI workshop on several fronts.⁴ Section 2 presents a derivation of the full governing equations from first principles. Separately, Section 3 examined different scaling regimes that yield reductions of the governing equations (1.1ab). Section 4 considers one of those cases and examines the forms of analytical problems that result from different forms of precast shell shapes with a particular choice for the thermal stresses. Continuing in exploring analytical approaches, section 5 considers how to describe boundary layers that could occur with rapid variations in the stress or deflection at the edges of between regions with smooth, slowly-varying behavior. Section 6 considered the one-dimensional analogue, the problem of a curved beam subject to thermal stresses, which was helpful for understanding how the stresses enter into both the governing equation and the boundary conditions. Returning to the full two-dimensional problem, section 7 outlines two classes of computational methods that can be applied. Finally, section 8 some brief considerations on how to approach the inverse problems described above can be accomplished once methods for solving the forward problem are set up.

2 Derivation of the governing equations

A systematic derivation of the equations of motion for the shell requires three interrelated concepts.⁵ First, a determination should be made how spatial variations in the displacement field generate strain. Second, a constitutive relation is proposed to relate the stress to the strain which in our case is then averaged over the thickness of the shell to generate a force per unit length. Finally, a force and momentum balance provides the equation of motion.

2.1 Strain and incompatibility with linear elasticity

Consider a pre-cast elastic shell with a small curvature and centre-surface given by $z = w_0(x, y)$ that undergoes a displacement from

$$\vec{X}(x, y, z) = \begin{pmatrix} x \\ y \\ z + w_0(x, y) \end{pmatrix} \quad \text{to} \quad \vec{x}(x, y, z) = \begin{pmatrix} x + u(x, y, z) \\ y + v(x, y, z) \\ z + w_0(x, y) + w(x, y, z) \end{pmatrix}. \quad (2.1)$$

⁴Some information on contributors to each section will be given to aid for any later follow-up contacts.

⁵This section is from work by Sean Bohun.

With this formulation a point near the centre surface $\vec{X} + \delta\vec{X}$ with

$$\begin{aligned}\delta\vec{X} &= \begin{pmatrix} \delta x \\ \delta y \\ \delta z + w_0(x + \delta x, y + \delta y) - w_0(x, y) \end{pmatrix} \\ &= \begin{pmatrix} 1 \\ 0 \\ \partial w_0(x, y)/\partial x \end{pmatrix} \delta x + \begin{pmatrix} 0 \\ 1 \\ \partial w_0(x, y)/\partial y \end{pmatrix} \delta y + \begin{pmatrix} 0 \\ 0 \\ 1 \end{pmatrix} \delta z + \mathcal{O}(\|\delta\vec{X}\|^2)\end{aligned}\quad (2.2)$$

is deformed to $\vec{x} + \delta\vec{x}$ with

$$\delta\vec{x} = \begin{pmatrix} u(x + \delta x, y + \delta y, z + \delta z) - u(x, y, z) \\ v(x + \delta x, y + \delta y, z + \delta z) - v(x, y, z) \\ w_0(x + \delta x, y + \delta y) - w_0(x, y) + w(x + \delta x, y + \delta y, z + \delta z) - w(x, y, z) \end{pmatrix}.\quad (2.3)$$

Computing the square of the change in length and keeping only the leading order terms allows one to identify

$$\frac{1}{2} (\|\delta\vec{x}\|^2 - \|\delta\vec{X}\|^2) = e_{xx} dx^2 + e_{yy} dy^2 + e_{zz} dz^2 + 2(e_{yz} dy dz + e_{xz} dx dz + e_{xy} dx dy)\quad (2.4)$$

with

$$e_{xx} = \frac{\partial u}{\partial x} + \frac{\partial w_0}{\partial x} \frac{\partial w}{\partial x} + \frac{1}{2} \left(\frac{\partial w}{\partial x} \right)^2 + \frac{1}{2} \left(\frac{\partial u}{\partial x} \right)^2 + \frac{1}{2} \left(\frac{\partial v}{\partial x} \right)^2,\quad (2.5a)$$

$$e_{yy} = \frac{\partial v}{\partial y} + \frac{\partial w_0}{\partial y} \frac{\partial w}{\partial y} + \frac{1}{2} \left(\frac{\partial w}{\partial y} \right)^2 + \frac{1}{2} \left(\frac{\partial u}{\partial y} \right)^2 + \frac{1}{2} \left(\frac{\partial v}{\partial y} \right)^2,\quad (2.5b)$$

$$e_{zz} = \frac{\partial w}{\partial z} + \frac{1}{2} \left(\frac{\partial w}{\partial z} \right)^2 + \frac{1}{2} \left(\frac{\partial u}{\partial z} \right)^2 + \frac{1}{2} \left(\frac{\partial v}{\partial z} \right)^2,\quad (2.5c)$$

$$e_{yz} = \frac{1}{2} \left(\frac{\partial w}{\partial y} + \frac{\partial v}{\partial z} + \frac{\partial w}{\partial y} \frac{\partial w}{\partial z} + \frac{\partial w_0}{\partial x} \frac{\partial w}{\partial z} + \frac{\partial u}{\partial y} \frac{\partial u}{\partial z} + \frac{\partial v}{\partial y} \frac{\partial v}{\partial z} \right),\quad (2.5d)$$

$$e_{xz} = \frac{1}{2} \left(\frac{\partial w}{\partial x} + \frac{\partial u}{\partial z} + \frac{\partial w}{\partial x} \frac{\partial w}{\partial z} + \frac{\partial w_0}{\partial y} \frac{\partial w}{\partial z} + \frac{\partial u}{\partial x} \frac{\partial u}{\partial z} + \frac{\partial v}{\partial x} \frac{\partial v}{\partial z} \right),\quad (2.5e)$$

$$e_{xy} = \frac{1}{2} \left(\frac{\partial u}{\partial y} + \frac{\partial v}{\partial x} + \frac{\partial w}{\partial x} \frac{\partial w}{\partial y} + \frac{\partial w_0}{\partial x} \frac{\partial w}{\partial y} + \frac{\partial w_0}{\partial y} \frac{\partial w}{\partial x} + \frac{\partial u}{\partial x} \frac{\partial u}{\partial y} + \frac{\partial v}{\partial x} \frac{\partial v}{\partial y} \right).\quad (2.5f)$$

To estimate the relative size of the various terms a scaling of the coordinates is introduced according to

$$x = L\tilde{x}, \quad y = L\tilde{y}, \quad z = h\tilde{z}, \quad u = \tilde{u}, \quad v = \tilde{v}, \quad w = \tilde{w}\tilde{w}_0\quad (2.6)$$

where L is a characteristic lateral length scale, not necessarily the size of the complete sheet of glass. The shear components (2.5d) and (2.5e) indicate that for balance, $\partial w/\partial x \sim \partial u/\partial z$ and $\partial w/\partial y \sim \partial v/\partial z$ so that $\tilde{u} \sim \tilde{v} \sim h\tilde{w}/L = \epsilon\tilde{w}$ where $\epsilon = h/L \ll 1$. If one further supposes that transverse displacements from the initial shell position are comparable in magnitude to the shell thickness then $\tilde{w} \sim h$. Finally, we set the characteristic length associated with the vertical variation of the shell as \mathcal{W} so that $w_0 = \mathcal{W}\tilde{w}_0 = \epsilon_0 L\tilde{w}_0$ with $\epsilon_0 = \mathcal{W}/L \ll 1$ independent of ϵ . Under these suppositions, we see that

$$(x, y, z, u, v, w, w_0) = L(\tilde{x}, \tilde{y}, \epsilon\tilde{z}, \epsilon^2\tilde{u}, \epsilon^2\tilde{v}, \epsilon\tilde{w}, \epsilon_0\tilde{w}_0)\quad (2.7)$$

where the tilde quantities are of order one. This set of scalings will act as a guide to determine the relative magnitude of the terms that will be encountered in the next phase of the derivation.

At this point we impose that the variation of the displacements u, v, w with the vertical position z is weak and so to this end we let, allowing for a mild abuse of notation,

$$u(x, y, z) = u(x, y) + z\beta_1(x, y) + \mathcal{O}(z^2) = u(x, y) - z\frac{\partial w}{\partial x} + \mathcal{O}(z^2),\quad (2.8a)$$

$$v(x, y, z) = v(x, y) + z\beta_2(x, y) + \mathcal{O}(z^2) = v(x, y) - z\frac{\partial w}{\partial y} + \mathcal{O}(z^2),\quad (2.8b)$$

$$w(x, y, z) = w(x, y) + \mathcal{O}(z^2),\quad (2.8c)$$

where β_1, β_2 and the form of w are chosen to eliminate the $\mathcal{O}(\epsilon)$ terms of e_{xz} , e_{yz} and e_{zz} . For each component of the strain we keep only terms of $\mathcal{O}(\epsilon^p)$, $\mathcal{O}(\epsilon^{p+1})$ and $\mathcal{O}(\epsilon\epsilon_0)$ where $p = 2$ for $\{e_{xx}, e_{yy}, e_{xy}\}$; $p = 1$ for $\{e_{yz}, e_{xz}\}$; and $p = 0$ for e_{zz} so that

$$e_{xx} = \frac{\partial u}{\partial x} - z \frac{\partial^2 w}{\partial x^2} + \frac{1}{2} \left(\frac{\partial w}{\partial x} \right)^2 + \frac{\partial w_0}{\partial x} \frac{\partial w}{\partial x} + \mathcal{O}(\epsilon^4), \quad (2.9a)$$

$$e_{yy} = \frac{\partial v}{\partial y} - z \frac{\partial^2 w}{\partial y^2} + \frac{1}{2} \left(\frac{\partial w}{\partial y} \right)^2 + \frac{\partial w_0}{\partial y} \frac{\partial w}{\partial y} + \mathcal{O}(\epsilon^4), \quad (2.9b)$$

$$e_{zz} = 0 + \mathcal{O}(\epsilon^2), \quad (2.9c)$$

$$e_{yz} = 0 + \mathcal{O}(\epsilon^3), \quad (2.9d)$$

$$e_{xz} = 0 + \mathcal{O}(\epsilon^3), \quad (2.9e)$$

$$e_{xy} = \frac{1}{2} \left(\frac{\partial u}{\partial y} + \frac{\partial v}{\partial x} - 2z \frac{\partial^2 w}{\partial x \partial y} + \frac{\partial w}{\partial x} \frac{\partial w}{\partial y} + \frac{\partial w_0}{\partial x} \frac{\partial w}{\partial y} + \frac{\partial w_0}{\partial y} \frac{\partial w}{\partial x} \right) + \mathcal{O}(\epsilon^4). \quad (2.9f)$$

Some clarity about the $\mathcal{O}(\epsilon^p)$ notation may be required at this point. In expression (2.9a), the $\mathcal{O}(\epsilon^4)$ denotes the contribution from

$$\frac{1}{2} \left(\frac{\partial u}{\partial x} \right)^2 + \frac{1}{2} \left(\frac{\partial v}{\partial x} \right)^2$$

listed in (2.5a) which has a relative size of $\mathcal{O}(\epsilon^4)$ according to (2.7). At this point the higher order terms are dropped.

The in-plane displacements (u, v) can be eliminated from (2.9) with the combination

$$\begin{aligned} -\frac{\partial^2 e_{xx}}{\partial y^2} + 2 \frac{\partial^2 e_{xy}}{\partial x \partial y} - \frac{\partial^2 e_{yy}}{\partial x^2} &= \frac{\partial^2 w_0}{\partial x^2} \frac{\partial^2 w}{\partial y^2} - 2 \frac{\partial^2 w_0}{\partial x \partial y} \frac{\partial^2 w}{\partial x \partial y} + \frac{\partial^2 w_0}{\partial y^2} \frac{\partial^2 w}{\partial x^2} + \frac{\partial^2 w}{\partial x^2} \frac{\partial^2 w}{\partial y^2} - \left(\frac{\partial^2 w}{\partial x \partial y} \right)^2 \\ &= K_G(w_0 + w) - K_G(w_0) \end{aligned} \quad (2.10)$$

where

$$K_G(w) = \frac{\partial^2 w}{\partial x^2} \frac{\partial^2 w}{\partial y^2} - \left(\frac{\partial^2 w}{\partial x \partial y} \right)^2 \quad (2.11)$$

is closely related to the Gaussian curvature.⁶ Consider the synclastic surface $w_{0a} = \frac{\beta}{2}(x^2 + y^2)$ and the anticlastic surface $w_{0b} = \beta xy$.⁷ A quick calculation shows that $K_G(w_{0a}) = \beta^2$ and $K_G(w_{0b}) = -\beta^2$, both constant, whereas the Gaussian curvatures of these surfaces are $\pm\beta^2(1 + \beta^2 x^2 + \beta^2 y^2)^{-2}$ respectively and not constant.

It is important to point out that for *linear* elasticity, (2.10) is identically zero reflecting the property that a flat sheet can be deformed without stretching only into a sheet with zero Gaussian curvature. This linear elasticity property can now be generalized to the observation that it is changes in K_G that generate nontrivial in-plane strains.

2.2 Linear stress-strain and averaging

To connect the in-plane strain to the in-plane stress we assume an isotropic material with small displacements so that the standard stress-strain relationships

$$e_{xx} = \frac{1}{E}(\sigma_{xx} - \nu\sigma_{yy}) + e_{xx}^0, \quad \sigma_{xx} = \frac{E}{1 - \nu^2} (e_{xx} + \nu e_{yy} - (e_{xx}^0 + \nu e_{yy}^0)), \quad (2.12a)$$

$$e_{yy} = \frac{1}{E}(\sigma_{yy} - \nu\sigma_{xx}) + e_{yy}^0, \quad \sigma_{yy} = \frac{E}{1 - \nu^2} (e_{yy} + \nu e_{xx} - (e_{yy}^0 + \nu e_{xx}^0)), \quad (2.12b)$$

$$e_{xy} = \frac{1}{E}(1 + \nu)\sigma_{xy} + e_{xy}^0, \quad \sigma_{xy} = \frac{E}{1 + \nu}(e_{xy} - e_{xy}^0), \quad (2.12c)$$

apply where E is the Young's modulus and ν is the Poisson ratio. Also included is a residual strain field with components $\{e_{xx}^0, e_{xy}^0, e_{yy}^0\}$. For thermal strain due to a temperature field, T , one would have

$$e_{xx}^0 = \alpha T, \quad e_{xy}^0 = 0, \quad e_{yy}^0 = \alpha T, \quad (2.13)$$

⁶The Gaussian curvature is given by $K_G(w)/(1 + w_x^2 + w_y^2)^2$, which reduces to curvature $\sim K_G(w)$ if $|\nabla w| \ll 1$.

⁷Synclastic — curved toward the same side in all directions (positive Gaussian curvature); Anticlastic — having opposite curvatures at given point (negative Gaussian curvature).

where α is a linear expansion coefficient. The in-plane stresses per unit length are found by integrating over the thickness of the shell.⁸ Denoting

$$S_{ij} = \int_{-h/2}^{h/2} \sigma_{ij} \, dz, \quad S_{ij}^{e0} = E \int_{-h/2}^{h/2} e_{ij}^0(x, y, z) \, dz \quad (2.14)$$

respectively as the i th component of the in-plane force per unit length acting on a section of shell with an outward unit normal in the j -direction and the various components of the averaged external strain. We find from (2.9), (2.12) and (2.14) that

$$\int_{-h/2}^{h/2} e_{xx} \, dz = \frac{1}{E} (S_{xx} - \nu S_{yy} + S_{xx}^{e0}) = h \left(\frac{\partial u}{\partial x} + \frac{1}{2} \left(\frac{\partial w}{\partial x} \right)^2 + \frac{\partial w_0}{\partial x} \frac{\partial w}{\partial x} \right), \quad (2.15a)$$

$$\int_{-h/2}^{h/2} e_{yy} \, dz = \frac{1}{E} (S_{yy} - \nu S_{xx} + S_{yy}^{e0}) = h \left(\frac{\partial v}{\partial y} + \frac{1}{2} \left(\frac{\partial w}{\partial y} \right)^2 + \frac{\partial w_0}{\partial y} \frac{\partial w}{\partial y} \right), \quad (2.15b)$$

$$\int_{-h/2}^{h/2} e_{xy} \, dz = \frac{1}{E} ((1 + \nu)S_{xy} + S_{xy}^{e0}) = \frac{h}{2} \left(\frac{\partial u}{\partial y} + \frac{\partial v}{\partial x} + \frac{\partial w}{\partial x} \frac{\partial w}{\partial y} + \frac{\partial w_0}{\partial x} \frac{\partial w}{\partial y} + \frac{\partial w_0}{\partial y} \frac{\partial w}{\partial x} \right). \quad (2.15c)$$

Note that we have invoked Saint-Venant's principle by imposing that

$$\int_{-h/2}^{h/2} \sigma_{zz} \, dz = 0 \quad (2.16)$$

which gives rise to a $\mathcal{O}(\epsilon^2)$ correction to (2.9c), preserving $e_{zz} = 0$ to $\mathcal{O}(\epsilon)$. Solving (2.15) for the S_{ij} generalizes the results on page 381 of Boley & Weiner [4] to

$$S_{xx} = \frac{Eh}{1 - \nu^2} \left(\frac{\partial u}{\partial x} + \frac{1}{2} \left(\frac{\partial w}{\partial x} \right)^2 + \frac{\partial w_0}{\partial x} \frac{\partial w}{\partial x} + \nu \left(\frac{\partial v}{\partial y} + \frac{1}{2} \left(\frac{\partial w}{\partial y} \right)^2 + \frac{\partial w_0}{\partial y} \frac{\partial w}{\partial y} \right) \right) - \frac{1}{1 - \nu^2} (S_{xx}^{e0} + \nu S_{yy}^{e0}), \quad (2.17a)$$

$$S_{yy} = \frac{Eh}{1 - \nu^2} \left(\frac{\partial v}{\partial y} + \frac{1}{2} \left(\frac{\partial w}{\partial y} \right)^2 + \frac{\partial w_0}{\partial y} \frac{\partial w}{\partial y} + \nu \left(\frac{\partial u}{\partial x} + \frac{1}{2} \left(\frac{\partial w}{\partial x} \right)^2 + \frac{\partial w_0}{\partial x} \frac{\partial w}{\partial x} \right) \right) - \frac{1}{1 - \nu^2} (S_{yy}^{e0} + \nu S_{xx}^{e0}), \quad (2.17b)$$

$$S_{xy} = \frac{Eh}{2(1 + \nu)} \left(\frac{\partial u}{\partial y} + \frac{\partial v}{\partial x} + \frac{\partial w}{\partial x} \frac{\partial w}{\partial y} + \frac{\partial w_0}{\partial x} \frac{\partial w}{\partial y} + \frac{\partial w_0}{\partial y} \frac{\partial w}{\partial x} \right) - \frac{1}{1 + \nu} S_{xy}^{e0}. \quad (2.17c)$$

The bending moment, M_{ij} , denotes the i th component of the moment per unit length acting on a section with outward normal in the direction j . Infinitesimal elements of these bending moments arise from the torque of the in-plane stress acting throughout the thickness of the shell. These internal torques take the form $\vec{\tau} = \vec{r} \times \vec{F}$ where \vec{r} is the position vector of a point being acted on by the force \vec{F} . Resolving into the various coordinate directions for a segment of shell one has

$$dM_{xx} \hat{\mathbf{i}} = z \hat{\mathbf{k}} \times \sigma_{xy} \, dz \hat{\mathbf{j}}, \quad dM_{yy} \hat{\mathbf{j}} = z \hat{\mathbf{k}} \times \sigma_{yx} \, dz \hat{\mathbf{i}}, \quad (2.18a)$$

$$dM_{xy} \hat{\mathbf{i}} = z \hat{\mathbf{k}} \times \sigma_{yy} \, dz \hat{\mathbf{j}}, \quad dM_{yx} \hat{\mathbf{j}} = z \hat{\mathbf{k}} \times \sigma_{xx} \, dz \hat{\mathbf{i}} \quad (2.18b)$$

so that

$$M_{xx} = - \int_{-h/2}^{h/2} \sigma_{xy} z \, dz, \quad M_{yy} = -M_{xx} = \int_{-h/2}^{h/2} \sigma_{xy} z \, dz, \quad (2.18c)$$

$$M_{xy} = - \int_{-h/2}^{h/2} \sigma_{yy} z \, dz, \quad M_{yx} = \int_{-h/2}^{h/2} \sigma_{xx} z \, dz. \quad (2.18d)$$

⁸The integration is computed about the centreline position of the shell, $z = w_0(x, y)$.

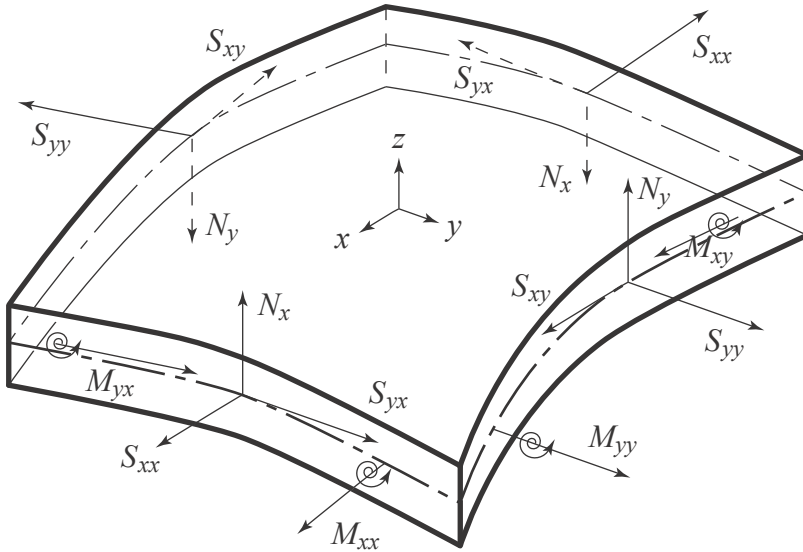


Figure 2.1: The in-plane, transverse and bending moments per unit length acting on a portion of shell.

Using (2.9), (2.12) and now (2.18), one finds

$$\int_{-h/2}^{h/2} e_{xx} z \, dz = \frac{1}{E} (M_{yx} + \nu M_{xy} + M_{xx}^{e0}) = -\frac{h^3}{12} \frac{\partial^2 w}{\partial x^2}, \quad (2.19a)$$

$$\int_{-h/2}^{h/2} e_{yy} z \, dz = \frac{1}{E} (-M_{xy} - \nu M_{yx} + M_{yy}^{e0}) = -\frac{h^3}{12} \frac{\partial^2 w}{\partial y^2}, \quad (2.19b)$$

$$\int_{-h/2}^{h/2} e_{xy} z \, dz = \frac{1}{E} ((1 + \nu) M_{yy} + M_{xy}^{e0}) = -\frac{h^3}{12} \frac{\partial^2 w}{\partial x \partial y}, \quad (2.19c)$$

where

$$M_{ij}^{e0} = E \int_{-h/2}^{h/2} e_{ij}^0(x, y, z) z \, dz \quad (2.20)$$

and consequently

$$M_{xx} = -M_{yy} = \frac{Eh^3}{12(1 + \nu)} \frac{\partial^2 w}{\partial x \partial y} + \frac{1}{1 + \nu} M_{xy}^{e0}, \quad (2.21a)$$

$$M_{xy} = \frac{Eh^3}{12(1 - \nu^2)} \left(\frac{\partial^2 w}{\partial y^2} + \nu \frac{\partial^2 w}{\partial x^2} \right) + \frac{1}{1 - \nu^2} (M_{yy}^{e0} + \nu M_{xx}^{e0}), \quad (2.21b)$$

$$M_{yx} = -\frac{Eh^3}{12(1 - \nu^2)} \left(\frac{\partial^2 w}{\partial x^2} + \nu \frac{\partial^2 w}{\partial y^2} \right) - \frac{1}{1 - \nu^2} (M_{xx}^{e0} + \nu M_{yy}^{e0}). \quad (2.21c)$$

2.3 Force and momentum balance

Figure 2.1 shows the in-plane, transverse and bending moments per unit length for a segment of shell with their appropriate sign conventions. Note that the two transverse shears per unit length are defined as

$$N_x = \int_{-h/2}^{h/2} \sigma_{xz} \, dz, \quad N_y = \int_{-h/2}^{h/2} \sigma_{yz} \, dz. \quad (2.22)$$

Since there is no acceleration in either the x or y direction and no rotational acceleration about these axes, balancing the forces we find

$$\frac{\partial S_{xx}}{\partial x} + \frac{\partial S_{xy}}{\partial y} = 0, \quad \frac{\partial S_{yx}}{\partial x} + \frac{\partial S_{yy}}{\partial y} = 0, \quad (2.23a)$$

which is automatically satisfied if we define an Airy stress potential φ so that

$$S_{xx} = \frac{\partial^2 \varphi}{\partial y^2}, \quad S_{xy} = -\frac{\partial^2 \varphi}{\partial x \partial y}, \quad S_{yy} = \frac{\partial^2 \varphi}{\partial x^2}, \quad (2.23b)$$

whereas, balancing the moments gives

$$\frac{\partial M_{xx}}{\partial x} + \frac{\partial M_{xy}}{\partial y} + N_y = 0, \quad \frac{\partial M_{yy}}{\partial y} + \frac{\partial M_{yx}}{\partial x} - N_x = 0. \quad (2.24)$$

Applying (2.15) and (2.23) to the operator (2.10) yields

$$-\frac{\partial^2 e_{xx}}{\partial y^2} + 2\frac{\partial^2 e_{xy}}{\partial x \partial y} - \frac{\partial^2 e_{yy}}{\partial x^2} = -\frac{1}{Eh} \left(\frac{\partial^4 \varphi}{\partial x^4} + 2\frac{\partial^4 \varphi}{\partial x^2 \partial y^2} + \frac{\partial^4 \varphi}{\partial y^4} + \frac{\partial^2 S_{xx}^{e0}}{\partial y^2} - 2\frac{\partial^2 S_{xy}^{e0}}{\partial x \partial y} + \frac{\partial^2 S_{yy}^{e0}}{\partial x^2} \right). \quad (2.25)$$

which connects the in-plane stress components to the changes in the shell curvature. Equating (2.10) and (2.25) gives the compatibility equation

$$\begin{aligned} -\frac{1}{Eh} \left(\frac{\partial^4 \varphi}{\partial x^4} + 2\frac{\partial^4 \varphi}{\partial x^2 \partial y^2} + \frac{\partial^4 \varphi}{\partial y^4} \right) &= \frac{1}{Eh} \left(\frac{\partial^2 S_{xx}^{e0}}{\partial y^2} - 2\frac{\partial^2 S_{xy}^{e0}}{\partial x \partial y} + \frac{\partial^2 S_{yy}^{e0}}{\partial x^2} \right) \\ &+ \frac{\partial^2 w_0}{\partial x^2} \frac{\partial^2 w}{\partial y^2} - 2\frac{\partial^2 w_0}{\partial x \partial y} \frac{\partial^2 w}{\partial x \partial y} + \frac{\partial^2 w_0}{\partial y^2} \frac{\partial^2 w}{\partial x^2} + \frac{\partial^2 w}{\partial x^2} \frac{\partial^2 w}{\partial y^2} - \left(\frac{\partial^2 w}{\partial x \partial y} \right)^2. \end{aligned} \quad (2.26)$$

What remains is the resolution of the forces and moments in the z -direction. The symmetry $\sigma_{yx} = \sigma_{xy}$ and the inherited average, $S_{yx} = S_{xy}$, eliminates any moment about the z -axis and if we allow for both a gravitational body force and an external applied pressure P_{ext} then the transverse acceleration for the shell is given by

$$\rho h \frac{\partial^2 w}{\partial t^2} = P_{\text{ext}} - \rho g h + \frac{\partial}{\partial x} \left(N_x + S_{xx} \frac{\partial f}{\partial x} + S_{yx} \frac{\partial f}{\partial y} \right) + \frac{\partial}{\partial y} \left(N_y + S_{yy} \frac{\partial f}{\partial y} + S_{xy} \frac{\partial f}{\partial x} \right). \quad (2.27)$$

where $f = w_0 + w$ is the overall final deflection. Using (2.21) and (2.24) we note that

$$\begin{aligned} \frac{\partial N_x}{\partial x} + \frac{\partial N_y}{\partial y} &= \frac{\partial}{\partial x} \left(\frac{\partial M_{yy}}{\partial y} + \frac{\partial M_{yx}}{\partial x} \right) - \frac{\partial}{\partial y} \left(\frac{\partial M_{xx}}{\partial x} + \frac{\partial M_{xy}}{\partial y} \right) \\ &= -\frac{Eh^3}{12(1-\nu^2)} \left(\frac{\partial^4 w}{\partial x^4} + 2\frac{\partial^4 w}{\partial x^2 \partial y^2} + \frac{\partial^4 w}{\partial y^4} \right) \\ &\quad - \frac{1}{1-\nu^2} \left(\frac{\partial^2}{\partial x^2} (M_{xx}^{e0} + \nu M_{yy}^{e0}) + 2(1-\nu) \frac{\partial^2 M_{xy}^{e0}}{\partial x \partial y} + \frac{\partial^2}{\partial y^2} (M_{yy}^{e0} + \nu M_{xx}^{e0}) \right). \end{aligned} \quad (2.28)$$

Using this result in (2.27) gives the relationship

$$\begin{aligned} \rho h \frac{\partial^2 w}{\partial t^2} &= P_{\text{ext}} - \rho g h - \frac{Eh^3}{12(1-\nu^2)} \left(\frac{\partial^4 w}{\partial x^4} + 2\frac{\partial^4 w}{\partial x^2 \partial y^2} + \frac{\partial^4 w}{\partial y^4} \right) + S_{xx} \frac{\partial^2 f}{\partial x^2} + 2S_{xy} \frac{\partial^2 f}{\partial x \partial y} + S_{yy} \frac{\partial^2 f}{\partial y^2} \\ &\quad - \frac{1}{1-\nu^2} \left(\frac{\partial^2}{\partial x^2} (M_{xx}^{e0} + \nu M_{yy}^{e0}) + 2(1-\nu) \frac{\partial^2 M_{xy}^{e0}}{\partial x \partial y} + \frac{\partial^2}{\partial y^2} (M_{yy}^{e0} + \nu M_{xx}^{e0}) \right). \end{aligned} \quad (2.29)$$

Using this formulation, the stress potential φ and *equilibrium* transverse displacement w are determined from the pre-cast state w_0 and a residual stress field $\{e_{xx}^0, e_{xy}^0, e_{yy}^0\}$ with

$$\begin{aligned} -\frac{1}{Eh} \nabla^4 \varphi &= \left(\frac{\partial^2 w_0}{\partial x^2} \frac{\partial^2 w}{\partial y^2} - 2\frac{\partial^2 w_0}{\partial x \partial y} \frac{\partial^2 w}{\partial x \partial y} + \frac{\partial^2 w_0}{\partial y^2} \frac{\partial^2 w}{\partial x^2} \right) + \left(\frac{\partial^2 w}{\partial x^2} \frac{\partial^2 w}{\partial y^2} - \left(\frac{\partial^2 w}{\partial x \partial y} \right)^2 \right) \\ &\quad + \frac{1}{Eh} \left(\frac{\partial^2 S_{xx}^{e0}}{\partial y^2} - 2\frac{\partial^2 S_{xy}^{e0}}{\partial x \partial y} + \frac{\partial^2 S_{yy}^{e0}}{\partial x^2} \right), \end{aligned} \quad (2.30a)$$

$$\begin{aligned} \frac{Eh^3}{12(1-\nu^2)} \nabla^4 w &= P_{\text{ext}} + \left(\frac{\partial^2 w_0}{\partial x^2} \frac{\partial^2 \varphi}{\partial y^2} - 2\frac{\partial^2 w_0}{\partial x \partial y} \frac{\partial^2 \varphi}{\partial x \partial y} + \frac{\partial^2 w_0}{\partial y^2} \frac{\partial^2 \varphi}{\partial x^2} \right) + \left(\frac{\partial^2 w}{\partial x^2} \frac{\partial^2 \varphi}{\partial y^2} - 2\frac{\partial^2 w}{\partial x \partial y} \frac{\partial^2 \varphi}{\partial x \partial y} + \frac{\partial^2 w}{\partial y^2} \frac{\partial^2 \varphi}{\partial x^2} \right) \\ &\quad - \frac{1}{1-\nu^2} \left(\frac{\partial^2}{\partial x^2} (M_{xx}^{e0} + \nu M_{yy}^{e0}) + 2(1-\nu) \frac{\partial^2 M_{xy}^{e0}}{\partial x \partial y} + \frac{\partial^2}{\partial y^2} (M_{yy}^{e0} + \nu M_{xx}^{e0}) \right) - \rho g h, \end{aligned} \quad (2.30b)$$

which confirms the form of the expressions (1.1) in the introduction with the inclusion of the effects of a residual stress. If the edges of the plate are considered to be free of stress then along $\partial\Omega_x = \{(\pm L, y) : -L \leq y \leq L\}$, $S_{xx} = S_{xy} = M_{yx} = \partial M_{yx}/\partial x - \partial M_{xx}/\partial y = 0$ so that in terms of w and φ , the boundary conditions are

$$\frac{\partial^2 \varphi}{\partial y^2} = 0, \quad \frac{\partial^2 \varphi}{\partial x \partial y} = 0, \quad \frac{\partial^2 w}{\partial x^2} + \nu \frac{\partial^2 w}{\partial y^2} = 0, \quad \frac{\partial^3 w}{\partial x^3} + (2 - \nu) \frac{\partial^3 w}{\partial x \partial y^2} = 0, \quad (2.31a)$$

and on $\partial\Omega_y = \{(x, \pm L) : -L \leq x \leq L\}$, $S_{yx} = S_{yy} = M_{xy} = \partial M_{xy}/\partial y + \partial M_{yy}/\partial x = 0$ gives the boundary conditions

$$\frac{\partial^2 \varphi}{\partial x^2} = 0, \quad \frac{\partial^2 \varphi}{\partial x \partial y} = 0, \quad \frac{\partial^2 w}{\partial y^2} + \nu \frac{\partial^2 w}{\partial x^2} = 0, \quad \frac{\partial^3 w}{\partial y^3} + (2 - \nu) \frac{\partial^3 w}{\partial y \partial x^2} = 0. \quad (2.31b)$$

Note that the boundary conditions are carefully described in Howell, Kozyreff and Ockendon [8, Sects. 4.6.2 and 6.4], the recent papers from Batista [2, 3] and the references cited therein. In general, thermal stresses generate contributions to these boundary conditions [14, Sect. 2.2], but only in the case that T varies across the thickness of the plate; for $T = T(x, y)$, these additional terms vanish identically.

In summary, to solve for the equilibrium displacement of a shell given by $z = w_0(x, y)$ with a set of external strains $\{e_{xx}^0, e_{xy}^0, e_{yy}^0\}$, imposed pressure P_{ext} , and appropriate boundary conditions, one first computes the S_{ij}^{e0} and M_{ij}^{e0} and from these averaged moments, w and φ are then found by solving the coupled system (2.30). Armed with w and φ , the in-plane stresses can be found using (2.23b) from which (2.17) determines the in-plane displacements. Finally, the elements of the stress and strain tensors are then determined from (2.9) and (2.12).

2.4 The case of uniform heating

Some of the subtleties of the problem can be revealed by considering a uniformly heated ($T = \text{const}$) shell of the form $z = w_0(x, y) = \beta xy$ on a square domain $\Omega = [-L, L]^2$, so that $e_{xx}^0 = \alpha T, e_{xy}^0 = 0, e_{yy}^0 = \alpha T$, are constant. From (2.14) and (2.20),

$$S_{xx}^{e0} = S_{yy}^{e0} = \alpha E h T, \quad S_{xy}^{e0} = 0, \quad M_{xx}^{e0} = M_{xy}^{e0} = M_{yy}^{e0} = 0, \quad (2.32)$$

and in this case (2.30) reduces to

$$\left. \begin{aligned} -\frac{1}{Eh} \nabla^4 \varphi &= -2\beta \frac{\partial^2 w}{\partial x \partial y} + \frac{\partial^2 w}{\partial x^2} \frac{\partial^2 w}{\partial y^2} - \left(\frac{\partial^2 w}{\partial x \partial y} \right)^2 \\ \frac{Eh^3}{12(1-\nu^2)} \nabla^4 w &= -2\beta \frac{\partial^2 \varphi}{\partial x \partial y} + \frac{\partial^2 w}{\partial x^2} \frac{\partial^2 \varphi}{\partial y^2} - 2 \frac{\partial^2 w}{\partial x \partial y} \frac{\partial^2 \varphi}{\partial x \partial y} + \frac{\partial^2 w}{\partial y^2} \frac{\partial^2 \varphi}{\partial x^2} \end{aligned} \right\}, \quad (x, y) \in \Omega \quad (2.33)$$

where we have assumed no external applied pressure or gravitational field, $P_{\text{ext}} = 0, \rho g h = 0$.

Rescaling the lengths, displacements and stress potential as

$$x = L\tilde{x}, \quad y = L\tilde{y}, \quad w = \bar{w}\tilde{w}, \quad w_0 = \mathcal{W}\tilde{x}\tilde{y}, \quad \varphi = Eh^3\tilde{\varphi}, \quad (2.34)$$

with $\mathcal{W} = \beta L^2$ gives the non-dimensionalized equations

$$-\left(\frac{h}{\bar{w}}\right)^2 \nabla^4 \tilde{\varphi} = -2 \left(\frac{\mathcal{W}}{\bar{w}}\right) \frac{\partial^2 \tilde{w}}{\partial \tilde{x} \partial \tilde{y}} + \frac{\partial^2 \tilde{w}}{\partial \tilde{x}^2} \frac{\partial^2 \tilde{w}}{\partial \tilde{y}^2} - \left(\frac{\partial^2 \tilde{w}}{\partial \tilde{x} \partial \tilde{y}}\right)^2, \quad -1 < \tilde{x}, \tilde{y} < 1, \quad (2.35a)$$

$$\frac{1}{12(1-\nu^2)} \nabla^4 \tilde{w} = -2 \left(\frac{\mathcal{W}}{\bar{w}}\right) \frac{\partial^2 \tilde{\varphi}}{\partial \tilde{x} \partial \tilde{y}} + \frac{\partial^2 \tilde{w}}{\partial \tilde{x}^2} \frac{\partial^2 \tilde{\varphi}}{\partial \tilde{y}^2} - 2 \frac{\partial^2 \tilde{w}}{\partial \tilde{x} \partial \tilde{y}} \frac{\partial^2 \tilde{\varphi}}{\partial \tilde{x} \partial \tilde{y}} + \frac{\partial^2 \tilde{w}}{\partial \tilde{y}^2} \frac{\partial^2 \tilde{\varphi}}{\partial \tilde{x}^2}, \quad -1 < \tilde{x}, \tilde{y} < 1, \quad (2.35b)$$

with boundary conditions (2.31a) applied at $\tilde{x} = \pm 1$ and (2.31b) applied at $\tilde{y} = \pm 1$. Equations (2.35) illustrate the how the three length scales, h, \bar{w} , and \mathcal{W} determine the dominant behaviour. For ‘thick’ plates, characterized by $h \gg \max(\bar{w}, \mathcal{W})$, the stress potential satisfies the biharmonic equation, $\nabla^4 \tilde{\varphi} = 0$, with appropriate boundary conditions. In this case the in-plane stresses decouple from the out-of-plane displacement. As the thickness of the plate reduces $h \ll \bar{w}$, the compatibility condition (2.35a) becomes a homogeneous Monge-Ampère equation, which effectively constrains the transverse displacement to a developable surface.⁹ Within this reduced class of surfaces the in-plane stress is then found by solving (2.35b). The resolution of the apparent paradox in the introduction is the recognition that uniform heating of a significantly curved thin sheet may yield nontrivial in-plane stress.

⁹A surface is said to be developable if it can be characterized as the envelope of a one-parameter family of planes.

If one instead assume that the heating is uniform only through the sheet and can vary with position then $e_{xx}^0 = \alpha T(x, y)$, $e_{xy}^0 = 0$, $e_{yy}^0 = \alpha T(x, y)$ and from (2.14) and (2.20),

$$S_{xx}^{e0} = S_{yy}^{e0} = \alpha EhT(x, y), \quad S_{xy}^{e0} = 0, \quad M_{xx}^{e0} = M_{xy}^{e0} = M_{yy}^{e0} = 0, \quad (2.36)$$

and (2.30) reduces to (1.1). The important point is that the form of (1.1) is restricted to residual stress that takes the form of (2.36) and (2.30) is required for the general situation.

3 Scaling analysis of the model

The primary objective of this portion of the project was to gain an understanding of how initial out of plane deflections, thermal stresses, and shear forces affect the final deflection (shape), after cooling with free edges, when manufacturing large, thin, sheets of glass.¹⁰ The governing set of equations are:

$$\nabla^4 \varphi = -Eh(w_{0xx}w_{yy} - 2w_{0xy}w_{xy} + w_{0yy}w_{xx}) - Eh(w_{xx}w_{yy} - w_{xy}^2) - Eh\nabla^2(\alpha T) \quad (3.1a)$$

$$D\nabla^4 w = (w_{0xx}\varphi_{yy} - 2w_{0xy}\varphi_{xy} + w_{0yy}\varphi_{xx}) + (w_{xx}\varphi_{yy} - 2w_{xy}\varphi_{xy} + w_{yy}\varphi_{xx}), \quad (3.1b)$$

where subscripts denote partial derivatives. Defining the symmetric bilinear operator

$$[u, v] = u_{xx}v_{yy} - 2u_{xy}v_{xy} + u_{yy}v_{xx},$$

we can rewrite the equations more compactly as

$$\nabla^4 \varphi = -Eh[w_0, w] - \frac{1}{2}Eh[w, w] - Eh\nabla^2(\alpha T) \quad (3.2a)$$

$$D\nabla^4 w = [w_0, \varphi] + [w, \varphi]. \quad (3.2b)$$

Note that our unknowns in the above system (3.2) are the Airy stress function φ , representing internal stresses, and the final deflection w . These equations are coupled, fourth order, and non-linear in each of our unknowns. It's evident that attempting to solve these equations in their full form will prove to be a difficult task. The goal of this section is to scale the model and obtain a more manageable system. In other words we want to simplify and classify the system (3.2) by extracting the most significant terms based on fundamental assumptions about the scaling of the problem.

The equations as presented in (3.2) are stated in their dimensional form. Before we begin discussing the significance of each of the terms we should non-dimensionalize the system. This will allow us to examine the influence of each term without having to take into account the choice of physical units. In our scaling analysis we will first consider a simplification of the above model where the initial deflections $w_0(x, y)$ are zero, in other words an initially flat plate. In anticipation of this we will non-dimensionalize this simplified system first and the full system second.

3.1 Scaling with Zero Initial Deflection, $w_0(x, y) \equiv 0$

Under the assumption of zero initial deflections the above system (3.2) reduces to

$$\nabla^4 \varphi = -\frac{1}{2}Eh[w, w] - Eh\nabla^2(\alpha T) \quad (3.3a)$$

$$D\nabla^4 w = [w, \varphi]. \quad (3.3b)$$

To introduce non-dimensional counterparts for each of our variables (x, y, w, T, φ) we introduce the following characteristic scales

$$x, y \sim L, \quad w \sim W, \quad T \sim \tau, \quad \varphi \sim \Phi. \quad (3.4)$$

We can now define non-dimensional counterpart for each of our variables in the following way

$$x = Lx', \quad y = Ly', \quad w = Ww', \quad T = \tau T', \quad \varphi = \Phi\varphi' \quad (3.5)$$

where the primed variables are dimensionless. Substituting these into our model equations (3.3) we obtain the following dimensionless system

$$S\nabla^4 \varphi' = -\frac{1}{2}\delta^2 [w', w'] - \mathcal{T}\nabla^2 T' \quad (3.6a)$$

$$\left(\frac{\epsilon^2}{12(1-\nu^2)S} \right) \nabla^4 w' = [w', \varphi'] \quad (3.6b)$$

¹⁰From material by Ray Walsh and Peter Buchak

where $\epsilon = h/L$, $\delta = W/L$, $\mathcal{T} = \alpha\tau$, and $S = \Phi/(EhL^2)$.

To simplify the model we're going to assume that $\delta^2 \ll \mathcal{O}(1)$ this will remove the non-linear term from equation (3.6a). This assumption is quite reasonable in the sense that it only requires that $W^2 \ll L^2$ or that the scale of our deflection is much less than the length scale as would be the case when manufacturing large flat glass sheets. In order to maintain the thermal coupling in the first equation we now have to assume that $S \sim \mathcal{T}$ which sets the scaling for Φ . All other scales are set by the physical problem. Now looking at equation (3.6b) if $\epsilon \ll S$ or $\epsilon \gg S$ then we'll have either the left-hand side or right-hand side of (3.6b) equal to zero which under free boundary conditions will give zero solutions for w . The only other possible case would be for $\epsilon^2/[12(1-\nu^2)S] \sim \mathcal{O}(1)$ which implies that $\epsilon \gg \delta \Rightarrow W \ll h$, that is, the deflections would be negligible compared to the thickness. So under the assumption of an initially flat plate and that the scale of our deflection is much less than the length scale we have a consistent scaling which tells us that heating an initially flat plate causes no out of plane deflections as one might expect. Scalings which involved the inclusion of the non-linear term were not considered as our primary goal was to justify the elimination of the non-linear terms.

3.2 Scaling of the Full Model

To non-dimensionalize the full model (3.2a) and (3.2b) we introduce the additional characteristic scale

$$w_0 \sim W_0$$

allowing us to define the non-dimensional counterpart as

$$w_0 = W_0 w'_0.$$

Substituting this, along with the non-dimensional definitions from the previous section, into equations (3.2) we obtain the following non-dimensional system

$$R\nabla^4 \varphi' = -\epsilon[w'_0, w'] - \frac{1}{2}\epsilon^2[w', w'] - H\nabla^2 T' \quad (3.7a)$$

$$\left(\frac{\epsilon\mu^2}{12(1-\nu^2)R} \right) \nabla^4 w' = [w'_0, \varphi'] + \epsilon[w', \varphi'] \quad (3.7b)$$

where $\epsilon = W/W_0$, $\mu = h/W_0$, $R = \Phi/(EhW_0^2)$, and $H = \alpha\tau L^2/W_0^2$. Note that from here on, for ease of notation, the primes will be dropped and all variables assumed dimensionless.

As was done in the previous section our first assumption will be that $\epsilon \ll \mathcal{O}(1)$ that is the scale of our final deflections is much less than that of our initial deflections. This will allow us to drop the non-linear term in (3.7b). In order to have non-trivial internal stress φ , under free boundary conditions, we must now assume that $\epsilon\mu^2/[12(1-\nu^2)R] \sim \mathcal{O}(1) \Rightarrow R \sim \epsilon\mu^2/[12(1-\nu^2)]$. Now we'll consider two cases: first $\mu \ll \mathcal{O}(1)$ which corresponds to large amplitude initial deflections and second $\mu \sim \mathcal{O}(1)$ which corresponds to small amplitude initial deflections. The case for $\mu \gg \mathcal{O}(1)$ would correspond to an initially flat plate considered above. For the case of $\mu \ll \mathcal{O}(1)$ we must have that $H \sim \epsilon$ to maintain the thermal coupling. This tells us that $\alpha\tau \sim \epsilon W_0^2/L^2$ or in other words for consistency we must have small thermal stresses. To summarize, under the assumptions of $\epsilon \ll \mathcal{O}(1)$, small amplitude initial deflections and small thermal stresses our system reduces to

$$H\nabla^2 T + \epsilon[w_0, w] = 0 \quad (3.8a)$$

$$\left(\frac{\epsilon\mu^2}{12(1-\nu^2)R} \right) \nabla^4 w - [w_0, \varphi] = 0. \quad (3.8b)$$

This is a second order system in each of our variables as (3.8a) can be solved for w and (3.8b) can be solved for φ . Unfortunately, since this system is second order there is an inconsistency with free boundary conditions providing evidence that there must exist a boundary layer in which the full non-linear system must be solved. For the second case, $\mu \sim \mathcal{O}(1)$, we must still have that $H \sim \epsilon$ to maintain the thermal coupling. This again implies small thermal stresses and the resultant system is as follows

$$R\nabla^4 \varphi = -\epsilon[w_0, w] - H\nabla^2 T \quad (3.9a)$$

$$\left(\frac{\epsilon\mu^2}{12(1-\nu^2)R} \right) \nabla^4 w = [w_0, \varphi]. \quad (3.9b)$$

If thermal stresses are not small, $H \gg \epsilon$, the assumption of our final deflection scale being much less than that of our initial deflections is inconsistent and the nonlinear terms must be kept.

4 Analytic calculations for fundamental precast shapes

In this section we examine the issues that arise in attempting to analytically solve the governing PDEs for a few very basic representative choices of the precast shell shape and the thermal stresses.¹¹ Following the presentation given by Howell et al. [8] in their section 4.8, we consider the linearized equations for weakly curved shells. In our notation, with the thermal stresses included, these equations are

$$\frac{1}{Eh} \nabla^4 \varphi = - \left(\frac{\partial^2 w_0}{\partial x^2} \frac{\partial^2 w}{\partial y^2} - 2 \frac{\partial^2 w_0}{\partial x \partial y} \frac{\partial^2 w}{\partial x \partial y} + \frac{\partial^2 w_0}{\partial y^2} \frac{\partial^2 w}{\partial x^2} \right) - \nabla^2(\alpha T), \quad (4.1a)$$

$$D \nabla^4 w = \frac{\partial^2 w_0}{\partial x^2} \frac{\partial^2 \varphi}{\partial y^2} - 2 \frac{\partial^2 w_0}{\partial x \partial y} \frac{\partial^2 \varphi}{\partial x \partial y} + \frac{\partial^2 w_0}{\partial y^2} \frac{\partial^2 \varphi}{\partial x^2}, \quad (4.1b)$$

with boundary conditions for unconstrained (free) edges to be described below.

We will assume given forms for $w_0(x, y)$ and $T(x, y)$ and use system (4.1ab) to obtain the Airy stress function $\varphi(x, y)$ and the additional deflection $w(x, y)$. This is essentially the “direct” or *forward* problem for the plate; the inverse problem of obtaining w_0 and/or T from measurements of the overall deflection $w + w_0$ will be briefly mentioned later.

The solution process will make use of an assumption that the E coefficient is large in order to treat (4.1a) as a singularly perturbed equation. The resulting analytical solutions are therefore slowly-varying outer solutions and will not typically be able to satisfy imposed boundary conditions without incorporating boundary layers.

4.1 Calculation for a synclastic shell

We begin by consider a given precast (unstressed) shell shape that has a local maximum at the origin (in the center of the plate),

$$w_0(x, y) = A \left[1 - \left(\frac{x}{S} \right)^2 - \left(\frac{y}{S} \right)^2 \right] \quad A = 10\text{mm} \quad S = 1250\text{mm}, \quad (4.2a)$$

where the domain of the plate is $|x| \leq 750\text{mm}$ and $|y| \leq 1000\text{mm}$. Having a positive Gaussian curvature, this case is sometimes called a synclastic shell [8]. The thermal stress is taken to be

$$\alpha T = B \left[1 - \left(\frac{2x}{L} \right)^2 \right] \quad B = 2.3 \times 10^{-5} \quad L = 1500\text{mm} \quad (4.2b)$$

We note that the coefficient B was selected to make the magnitude of the thermal stress be of the same order as the Gaussian curvature of w_0 , namely $w_{0xx}w_{0yy} - w_{0xy}^2 = \nabla^2(\alpha T)$, yielding $B = O(A^2 L^2 / (4S^4))$.

The solution process proceeds in two steps given in the following two subsections.

4.1.1 Step 1: determining $w(x, y)$

Consider the equation for the Airy stress function, (4.1a) and substitute-in the analytic forms given in (4.2ab) to yield

$$\frac{1}{Eh} \nabla^4 \varphi = \frac{2A}{S^2} \nabla^2 w - \frac{8B}{L^2}. \quad (4.3)$$

Assuming that E is large, if φ is slowly varying and $O(1)$, then the biharmonic term on the left side of the equation is negligible, further reducing the equation to a simple Poisson equation for w , with constant forcing,

$$\nabla^2 w = \frac{4S^2 B}{L^2 A}. \quad (4.4)$$

The general solution of (4.4) can be separated into particular and homogeneous solutions and expressed as

$$w(x, y) = \frac{2S^2 B}{A} \left[\beta \left(\frac{x}{L} \right)^2 + (1 - \beta) \left(\frac{y}{L} \right)^2 \right] + \omega(x, y), \quad (4.5)$$

where ω is a harmonic function, satisfying Laplace’s equation, $\nabla^2 \omega = 0$, and β is a constant that corresponds to an orientational preference (x vs. y) in the solution, that might be due to boundary conditions or edge effects, with $\beta = \frac{1}{2}$ giving the symmetric form.

¹¹From material by Tom Witelski

4.1.2 Step 2: determining $\varphi(x, y)$

Having determined the form of $w(x, y)$ in Step 1, we now turn to using equation (4.1b). In this case, substituting (4.5) into the biharmonic operator on the left-side of (4.1b) vanishes since

$$D\nabla^2(\nabla^2 w) = D\nabla^2 \left(\frac{4S^2 B}{L^2 A} + 0 \right) = 0. \quad (4.6)$$

Consequently, after using (4.2a), equation (4.1b) reduces to Laplace's equation for the Airy stress function,

$$0 = -\frac{2A}{S^2} \nabla^2 \varphi. \quad (4.7)$$

4.1.3 Checking boundary conditions on $w(x, y)$

We briefly consider if the deflection (4.5) could satisfy the boundary conditions at a free edge (see [8, Eqn 4.6.19]); consider the conditions at the right boundary, $x = L/2$,

$$\frac{\partial^2 w}{\partial x^2} + \nu \frac{\partial^2 w}{\partial y^2} = 0, \quad \frac{\partial}{\partial x} \left[\frac{\partial^2 w}{\partial x^2} + (2 - \nu) \frac{\partial^2 w}{\partial y^2} \right] = 0. \quad (4.8)$$

Substituting (4.5) into the second boundary condition yields

$$\frac{\partial}{\partial x} \left(\frac{2S^2 B}{L^2 A} (2\beta + 2(1 - \beta)(2 - \nu)) + \omega_{xx} + (2 - \nu)\omega_{yy} \right) = 0 \quad \implies \quad \omega_{xxx} + (2 - \nu)\omega_{yyx} = 0. \quad (4.9)$$

Since ω is harmonic, $\omega_{xx} = -\omega_{yy}$, so this boundary condition reduces to $(1 - \nu)\omega_{yyx} = 0$ on the boundary $x = L/2$. Integrating along the boundary, we conclude that the normal derivative of ω would have to be linear along the boundary,

$$\left. \frac{\partial \omega}{\partial x} \right|_{x=L/2} = C_1 y + C_2, \quad (4.10)$$

with C_1, C_2 being two arbitrary constants.

Turning to the first boundary condition, substituting (4.5) yields

$$\frac{2S^2 B}{L^2 A} (2\beta + 2(1 - \beta)\nu) + \omega_{xx} + \nu\omega_{yy} = 0. \quad (4.11)$$

Again using the fact that ω is harmonic, we can reduce this further,

$$\left. \omega_{yy} \right|_{x=L/2} = \frac{1}{1 - \nu} \frac{2S^2 B}{L^2 A} (2\beta + 2(1 - \beta)\nu)$$

and after integrating along the boundary,

$$\left. \omega \right|_{x=L/2} = \frac{1}{1 - \nu} \frac{S^2 B}{L^2 A} (2\beta + 2(1 - \beta)\nu) y^2 + C_3 y + C_4, \quad (4.12)$$

with C_3, C_4 being two additional arbitrary constants of integration. The fact that ω is harmonic does not seem to impose further constraints relating these constants.

Boundary conditions of the same form (4.8) also apply at the left edge of the plate, $x = -L/2$ and the boundary conditions at the top and bottom edges ($y = \pm 1000\text{mm}$) are given by

$$\nu \frac{\partial^2 w}{\partial x^2} + \frac{\partial^2 w}{\partial y^2} = 0 \quad \frac{\partial}{\partial y} \left[\frac{\partial^2 w}{\partial y^2} + (2 - \nu) \frac{\partial^2 w}{\partial x^2} \right] = 0 \quad (4.13)$$

While (4.5) has harmonic function $\omega(x, y)$ and constant β as degrees of freedom, it seems unlikely that all of the free-edge boundary conditions could be satisfied by the outer solution, so we expect the need for boundary layers.

4.2 Calculation for an anticlastic shell

As a second example we consider the case of a precast shell shape having an inflection point, with w_0 given as a hyperbolic saddle,

$$w_0(x, y) = A \left[1 - \left(\frac{x}{S} \right)^2 + \left(\frac{y}{S} \right)^2 \right] \quad A = 10\text{mm} \quad S = 1250\text{mm} \quad (4.14a)$$

on the same plate domain and again with the same thermal stress,

$$\alpha T = B \left[1 - \left(\frac{2x}{L} \right)^2 \right] \quad B = 2.3 \times 10^{-5} \quad L = 1500\text{mm} \quad (4.14b)$$

In contrast to the first example (4.2), which had a positive constant Gaussian curvature, this choice of $w_0(x, y)$ has a negative constant Gaussian curvature and is called an anticlastic shell.

Proceeding as in the previous example, carrying out Step 1 reduces (4.1a) to

$$\frac{1}{Eh} \nabla^4 \varphi = \frac{2A}{S^2} (w_{xx} - w_{yy}) - \frac{8B}{L^2}.$$

Using the assumption that E is large, reduces this equation to an inhomogeneous wave equation for $w(x, y)$,

$$w_{xx} = w_{yy} + \frac{4S^2 B}{L^2 A}. \quad (4.15)$$

The general solution of this wave equation is

$$w(x, y) = \frac{2S^2 B}{A} \left[\beta \left(\frac{x}{L} \right)^2 - (1 - \beta) \left(\frac{y}{L} \right)^2 \right] + f(x - y) + g(x + y) \quad (4.16)$$

with f, g being arbitrary traveling wave profiles.

Using (4.14ab), Step 2 reduces (4.1b) to

$$D \nabla^4 w = -\frac{2A}{S^2} (\varphi_{xx} - \varphi_{yy}) \quad (4.17)$$

but in using (4.16) for $w(x, y)$, we note that the biharmonic term does not vanish in this case, but yields forcing terms due to the f, g functions,

$$D (f''''(x - y) + g''''(x + y)) = -\frac{2A}{S^2} (\varphi_{xx} - \varphi_{yy}). \quad (4.18)$$

This is another inhomogeneous wave equation, and hence the Airy stress function can also be expressed via D'Alembert solution.

4.3 Calculation for a higher-order anticlastic shell

The previous two examples considered the simplest non-trivial types of pre-cast deflections, characterized by having uniform constant Gaussian curvatures. The positive Gaussian curvature case yielded elliptic PDE problems in terms of the simplest elliptic operator (the Laplacian), while the negative Gaussian curvature case yielded hyperbolic PDE problems in terms of the linear wave equation. The following example is motivated by exploring how the analysis changes with first level spatial variation in the Gaussian curvature.

Consider the given precast shell shape (called a ‘‘monkey saddle’’ for its alternating three-hill/three-valley structure)

$$w_0(x, y) = A \left[1 - \left(\frac{x}{S} \right)^3 + 3 \frac{xy^2}{S^3} \right] \quad A = 10\text{mm} \quad S = 1250\text{mm} \quad (4.19)$$

on $|x| \leq 750\text{mm}$ and $|y| \leq 1000\text{mm}$. The monkey saddle has negative definite Gaussian curvature, being zero only at the origin,

$$K = w_{0xx} w_{0yy} - w_{0xy}^2 = -\frac{36A^2}{S^6} (x^2 + y^2).$$

We again take the same form of the thermal stress, (4.14b).

Following Step 1, we substitute $w_0, \alpha T$ into (4.1a) to yield

$$\frac{1}{Eh} \nabla^4 \varphi = \frac{6A}{S^3} (x[w_{xx} - w_{yy}] - 2yw_{xy}) - \frac{8B}{L^2}. \quad (4.20)$$

Again assuming E is large, equation (4.20) can be reduced to a second order PDE for the outer solution for $w(x, y)$,

$$x[w_{xx} - w_{yy}] - 2yw_{xy} = \frac{4S^2B}{L^2A}, \quad (4.21)$$

but this is a more complicated inhomogeneous equation with variable coefficients that cannot be solved in closed-form.

To take a step forward on constructing the overall solution, we seek a homogeneous solution of the second order PDE

$$x[w_{xx} - w_{yy}] - 2yw_{xy} = 0. \quad (4.22)$$

This equation can be analyzed by taking a Fourier transform of the solution¹²,

$$\hat{w}(k, \ell) = \frac{1}{4\pi^2} \iint w(x, y) e^{-i(kx + \ell y)} dx dy$$

to yield the transform of the PDE,

$$\frac{\partial}{\partial k} ([k^2 - \ell^2] \hat{w}) - 2 \frac{\partial}{\partial \ell} (k\ell \hat{w}) = 0 \quad \implies \quad (k^2 - \ell^2) \frac{\partial \hat{w}}{\partial k} - 2k\ell \frac{\partial \hat{w}}{\partial \ell} = 0. \quad (4.23)$$

We observe that in Fourier-transform-space, the PDE has been reduced to a first-order equation that can be solved in general using the method of characteristics as

$$\hat{w}(k, \ell) = f(\ell^2(\ell^2 - 3k^2)^2). \quad (4.24)$$

Obtaining $w(x, y)$ then involves the challenging problem of evaluating the inverse Fourier transform integral,

$$w(x, y) = \iint f(\ell^2(\ell^2 - 3k^2)^2) e^{i(kx + \ell y)} dk d\ell. \quad (4.25)$$

Further generalization are expected to yield even-more difficult analytical problems, consequently numerical methods may be a more practical approach in general.

5 Fourier transform analysis of the linearized problem

Due to the large size of the glass sheet ($L \approx 2\text{m}$) compared to the thickness $h = 0.5\text{mm}$, for deformations occurring away from the boundaries of the sheet, we can use Fourier transforms to analyze the behavior of the glass sheet, treating it as an infinite domain.¹³ We use a linear form of the equations given by

$$-\nabla^4 \varphi = Eh(w_{0xx}w_{yy} - 2w_{0xy}w_{xy} + w_{0yy}w_{xx}) + Eh\alpha \nabla^2 T, \quad (5.1a)$$

$$D\nabla^4 w = w_{0xx}\varphi_{yy} - 2w_{0xy}\varphi_{xy} + w_{0yy}\varphi_{xx} \quad (5.1b)$$

where φ represents the Airy stress function, w_0 the pre-stress shape, w the deflection from the pre-stress shape and T the change in temperature from shape state w_0 to $w_0 + w$. Physical constants E , α , h , and D represent the elastic modulus, thermal expansion coefficient, thickness of the glass plate, and plate stiffness respectively. We non dimensionalize the equations according to the scaling

$$x = Lx', \quad y = Ly', \quad w_0 = W_0w'_0, \quad w = \Omega_0w', \quad \varphi = (D\Omega_0/hW_0)\varphi', \quad T = \tau T'. \quad (5.2)$$

The nondimensional equations (5.1a) and (5.1b) become

$$-\delta \nabla^4 \varphi = w_{0xx}w_{yy} - 2w_{0xy}w_{xy} + w_{0yy}w_{xx} + \psi \nabla^2 T, \quad (5.3a)$$

$$\nabla^4 w = w_{0xx}\varphi_{yy} - 2w_{0xy}\varphi_{xy} + w_{0yy}\varphi_{xx} \quad (5.3b)$$

¹²Neglecting finite-domain effects for the moment to see how this analytical approach works out.

¹³From material by Aaron Bardall and Hangjie Ji

where the dimensionless parameters are given by

$$\delta = \frac{D}{EhW_0^2}, \quad \psi = \frac{\alpha\tau L^2}{\Omega_0 W_0}. \quad (5.4)$$

We introduce a scaling according to non-dimensional parameter δ of the form

$$\varphi = \delta^{-1/2}\bar{\varphi}, \quad (x, y) = \delta^{1/4}(\xi, \eta) \quad (5.5)$$

which introduces operator relations

$$\frac{\partial}{\partial x} = \delta^{-1/4}\frac{\partial}{\partial \xi}, \quad \frac{\partial}{\partial y} = \delta^{-1/4}\frac{\partial}{\partial \eta}, \quad \nabla^2 = \left(\frac{\partial^2}{\partial x^2} + \frac{\partial^2}{\partial y^2}\right) = \delta^{-1/2}\bar{\nabla}^2 = \delta^{-1/2}\left(\frac{\partial^2}{\partial \xi^2} + \frac{\partial^2}{\partial \eta^2}\right). \quad (5.6)$$

With this scaling imposed, the non dimensional equations (5.3a) and (5.3b) become

$$-\bar{\nabla}^4\bar{\varphi} = w_{0xx}w_{\eta\eta} - 2w_{0xy}w_{\xi\eta} + w_{0yy}w_{\xi\xi} + \psi\bar{\nabla}^2T, \quad (5.7a)$$

$$\bar{\nabla}^4w = w_{0xx}\bar{\varphi}_{\eta\eta} - 2w_{0xy}\bar{\varphi}_{\xi\eta} + w_{0yy}\bar{\varphi}_{\xi\xi}. \quad (5.7b)$$

In order to perform a transform, we first assign the pre-stress sheet deflection $w_0(x, y) = ax^2 + bxy + cy^2$. This reduces the scaled equations (5.7a) and (5.7b) to

$$-\bar{\nabla}^4\bar{\varphi} = 2(aw_{\eta\eta} - bw_{\xi\eta} + cw_{\eta\eta}) + \psi\bar{\nabla}^2T, \quad (5.8a)$$

$$\bar{\nabla}^4w = 2(a\bar{\varphi}_{\eta\eta} - b\bar{\varphi}_{\xi\eta} + c\bar{\varphi}_{\eta\eta}). \quad (5.8b)$$

We want to analyze the behavior of this system on an infinite domain, which will provide insight into the behavior over the bulk of the glass sheet not influenced by the boundary of the sheet. We assume that the non dimensional stress function $\bar{\varphi}$ and deflection w go to zero in the far field and employ a Fourier transform over the 2-D plane. We define our Fourier transform pair as given by

$$\hat{F}(u, v) = \iint_{\mathbb{R}^2} F(\xi, \eta)e^{-2\pi i u \xi}e^{-2\pi i v \eta} d\xi d\eta, \quad (5.9a)$$

$$F(\xi, \eta) = \iint_{\mathbb{R}^2} \hat{F}(u, v)e^{2\pi i u \xi}e^{2\pi i v \eta} du dv. \quad (5.9b)$$

Employing the forward transform given by (5.9a), our model (5.8a) and (5.8b) are represented algebraically in Fourier space as

$$(2\pi)^2(u^2 + v^2)^2\hat{\varphi} = 2(av^2 - buv + cu^2)\hat{w} + \psi(u^2 + v^2)\hat{T}, \quad (5.10a)$$

$$(2\pi)^2(u^2 + v^2)^2\hat{w} = -2(av^2 - buv + cu^2)\hat{\varphi} \quad (5.10b)$$

Algebraically solving (5.10a) and (5.10b) for transform variables we obtain

$$\hat{\varphi} = \frac{(2\pi)^2(u^2 + v^2)^3}{(2\pi)^4(u^2 + v^2)^4 + 4(av^2 - buv + cu^2)^2}\psi\hat{T}, \quad (5.11a)$$

$$\hat{w} = \frac{-2(u^2 + v^2)(av^2 - buv + cu^2)}{(2\pi)^4(u^2 + v^2)^4 + 4(av^2 - buv + cu^2)^2}\psi\hat{T}. \quad (5.11b)$$

We then wish to prescribe realistic temperature distribution that will satisfy our assumption that the stress function $\bar{\varphi}$ and deflection function ω go to zero. This requires the temperature in the spatial domain to decay to zero in the far field. A nondimensional temperature is assumed as

$$T(\xi, \eta) = e^{-r|\xi|}e^{-s|\eta|} \quad (5.12)$$

where r and s are positive constants. Transforming (5.12), we obtain

$$\begin{aligned} \hat{T} &= \iint_{\mathbb{R}^2} e^{-r|\xi|}e^{-s|\eta|}e^{-2\pi i u \xi}e^{-2\pi i v \eta} d\xi d\eta = \int_{\mathbb{R}} e^{-r|\xi|}e^{-2\pi i u \xi} d\xi \int_{\mathbb{R}} e^{-s|\eta|}e^{-2\pi i v \eta} d\eta \\ &= \left(\frac{2r}{r^2 + (2\pi u)^2}\right) \left(\frac{2s}{s^2 + (2\pi v)^2}\right) = \frac{4rs}{(r^2 + (2\pi u)^2)(s^2 + (2\pi v)^2)}. \end{aligned} \quad (5.13)$$

Under this temperature distribution and resulting transform given by (5.13), our transform variables of interest given by (5.11a) and (5.11b) become

$$\hat{\varphi}(u, v) = \frac{4rs(2\pi)^2(u^2 + v^2)^3\psi}{((2\pi)^4(u^2 + v^2)^4 + 4(av^2 - buv + cu^2)^2)(r^2 + (2\pi u)^2)(s^2 + (2\pi v)^2)}, \quad (5.14a)$$

$$\hat{w}(u, v) = \frac{-8rs(u^2 + v^2)(av^2 - buv + cu^2)\psi}{((2\pi)^4(u^2 + v^2)^4 + 4(av^2 - buv + cu^2)^2)(r^2 + (2\pi u)^2)(s^2 + (2\pi v)^2)}. \quad (5.14b)$$

Where the scaled solutions in the spatial domain are given by the inverse transform

$$\bar{\varphi}(\xi, \eta) = \iint_{\mathbb{R}^2} \hat{\varphi}(u, v) e^{2\pi i(u\xi + v\eta)} \, du \, dv, \quad (5.15a)$$

$$w(\xi, \eta) = \iint_{\mathbb{R}^2} \hat{w}(u, v) e^{2\pi i(u\xi + v\eta)} \, du \, dv. \quad (5.15b)$$

An asymptotic strategy for solving for variables $\bar{\varphi}(\xi, \eta)$ was developed using the method of steepest descent. According to the method, the largest asymptotic contribution for an integral of the form

$$I(z) = \int_C e^{zf(u)} g(u) \, du \quad (5.16)$$

comes from when $f(u)$ reaches a maximum value. Therefore we solve for u_0 such that $\text{Re}(f'(u_0)) = 0$ and the integral is then approximated by

$$I(z) \sim \frac{e^{zf(u_0)} g(u_0)}{\sqrt{-zf''(u_0)}} \quad (5.17)$$

as $z \rightarrow \infty$. We reformulate the transform variables given by (5.14a) and (5.14b) as

$$\hat{\varphi}(u, v) = \frac{4rs(2\pi)^2(u^2 + v^2)^3\psi}{(r^2 + (2\pi u)^2)(s^2 + (2\pi v)^2)} e^{-\log \mathcal{D}(u, v)}, \quad (5.18a)$$

$$\hat{w}(u, v) = \frac{-8rs(u^2 + v^2)(av^2 - buv + cu^2)\psi}{(r^2 + (2\pi u)^2)(s^2 + (2\pi v)^2)} e^{-\log \mathcal{D}(u, v)}, \quad (5.18b)$$

where

$$\mathcal{D}(u, v) = (2\pi)^4(u^2 + v^2)^4 + 4(av^2 - buv + cu^2)^2 \quad (5.19)$$

which recasts the integral (5.15a) as

$$\bar{\varphi}(\xi, \eta) \sim \int_{\mathbb{R}} -e^{f(u_0, v)} \frac{4rs(2\pi)^2(u_0^2 + v^2)^3\psi \left(f''(u_0, v) \right)^{-1/2}}{(r^2 + (2\pi u_0)^2)(s^2 + (2\pi v)^2)} e^{2\pi i v \eta} \, dv \quad (5.20)$$

with

$$f(u, v) = 2\pi i u \xi - \log(\mathcal{D}(u, v)). \quad (5.21)$$

This process can be repeated to solve for an approximation $\bar{\varphi}(\xi, \eta)$ for the integrand presented in (5.20), and the entire process can be repeated to solve for $w(\xi, \eta)$. Further work on this approach would involve approximation (steepest descent asymptotics) and interpretation of the results of these integrals [20].

6 Study of the one-dimensional beam analog

This section investigates a 1-D analog of the full shell problem in order to gain some fundamental insights on effects to be expected from thermoelasticity and thermal stresses.¹⁴ Taking a step back from the full problem of analyzing a plate or shell, we will now study problems for a one-dimensional beam on an elastic foundation. The spatially uniform elastic foundation considered in this basic model, with spring constant k , could be replaced by a spatially-varying coefficient $k(x)$ to try to represent a beam supported by contact with a finite number of individual pins, as in [1]. Two sets of boundary conditions (free-free and pinned-pinned) were applied to the beam, as well as two sets of initial conditions and two sets of temperature distributions.

¹⁴This section is from work by Michael Mazzoleni, Jared Little, Andrew deStefan, and Mahdi Bandegi

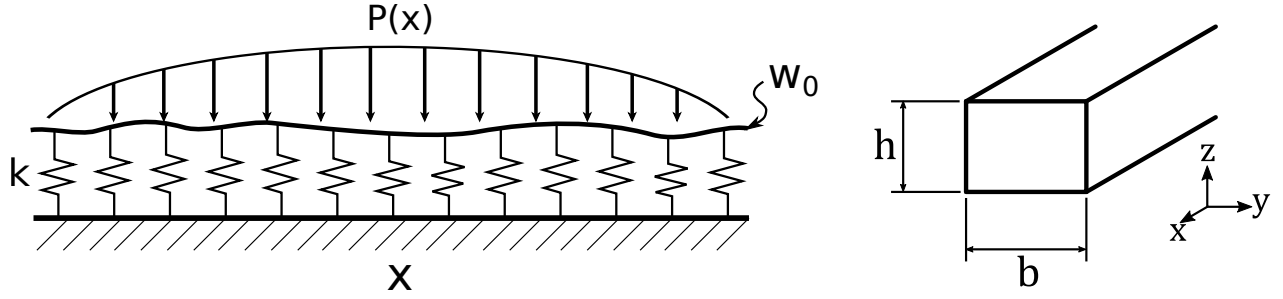


Figure 6.1: (Left) Schematic illustration of a beam with an initial shape w_0 and an applied load $P(x)$. The beam is resting on an elastic foundation with stiffness k . (Right) Schematic of the beam cross-section.

6.1 Problem Formulation

The beam is assumed to be resting on an elastic foundation with stiffness k and has an initial shape w_0 and an applied load $P(x)$, as illustrated in Fig. 6.1(Left). The beam is assumed to long and slender with length L , and the cross-section is defined in Fig. 6.1(Right).

The governing equation for this system was determined by coupling linear beam theory with thermoelastic effects. The equation also accounted for the initial shape of the beam and the elastic foundation that the beam rests upon. The governing equation is the fourth-order linear ordinary differential equation,

$$\frac{d^4 w}{dx^4} + \frac{k(w + w_0)}{EI} = \frac{P(x)}{EI} - \frac{\alpha}{I} \frac{d^2}{dx^2} \int_A T(x, z) z \, dA, \quad (6.1)$$

where w is the vertical perturbation of the beam from its initial shape, E is the elastic modulus of the beam, I is the area moment of inertia, and α is the coefficient of thermal expansion, see Theory of Elasticity and Thermal Stresses [5, Ch. 14, Eq. (14.138)]. In (6.1) the temperature distribution is integrated across the cross-section of the beam; In order to proceed, we must assume a temperature distribution $T(x, z)$. A realistic selection is

$$T(x, z) = \beta z T_o(x), \quad (6.2)$$

where β is a dimensionless scaling parameter and $T_o(x)$ is an arbitrary temperature function that varies in terms of x . The governing equation for the system can therefore be simplified by substituting Eq. (6.2) into Eq. (6.1) and evaluating the area integral, which results in

$$\frac{d^4 w}{dx^4} + \frac{k(w + w_0)}{EI} = \frac{P(x)}{EI} - \alpha \beta \frac{d^2 T_o(x)}{dx^2}. \quad (6.3)$$

The following scaling conventions were introduced for nondimensionalization.

$$w = L\tilde{w}, \quad x = L\tilde{x}, \quad P = \lambda\tilde{P}, \quad T_o = \chi\tilde{T}_o. \quad (6.4)$$

The resulting dimensionless governing equation is

$$\frac{d^4 \tilde{w}}{d\tilde{x}^4} + K(\tilde{w} + \tilde{w}_0) = \tilde{P} - \frac{d^2 \tilde{T}_o}{d\tilde{x}^2}, \quad 0 \leq \tilde{x} \leq 1, \quad (6.5)$$

with parameters

$$K = \frac{kL^4}{EI}, \quad \lambda = \frac{EI}{L^3}, \quad \chi = \frac{1}{\alpha\beta L}. \quad (6.6)$$

This model is linear, and given parameter values and functions $\tilde{w}_0(\tilde{x})$, $\tilde{P}(\tilde{x})$, $\tilde{T}_o(\tilde{x})$, analytical formulas for the solution can be written. However, numerical solution of this ODE are straightforward to set up using finite difference schemes and will generalize to the full two-dimensional problem.

6.2 Solutions

System (6.5) was analyzed for a variety of conditions to understand its behavior. Two sets of boundary conditions (free-free and pinned-pinned) were applied to the beam, as well as two choices for initial, press-stressed deflection \tilde{w}_0 and two examples of temperature distributions.

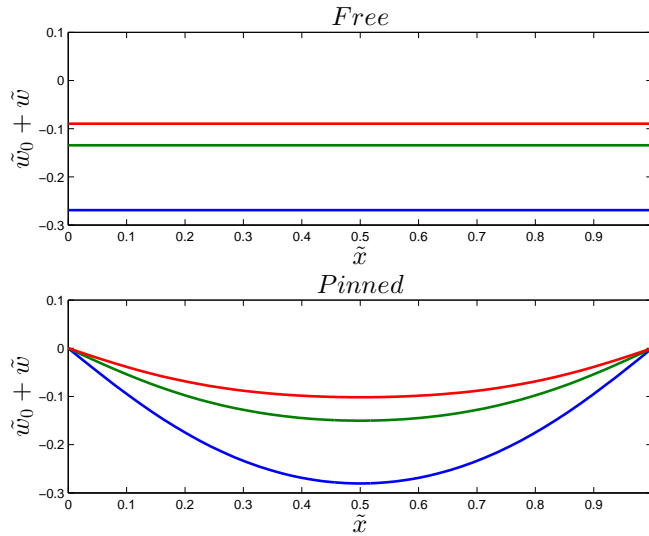


Figure 6.2: Solutions with free vs. pinned boundary conditions on a flat ($\tilde{w}_0 = 0$) beam with no imposed thermal stresses ($\tilde{T}_o = 0$), subject to uniform loading due to its weight ($\tilde{P} = -\rho b h g / \lambda$). Beam shapes are shown with various foundation stiffnesses: $K = 500$ (blue), $K = 1000$ (green), $K = 1500$ (red).

The one-dimensional version of the free-free boundary conditions are

$$\left. \begin{aligned} \frac{d^2 \tilde{w}}{d\tilde{x}^2} + \tilde{T}_o &= 0 \\ \frac{d^3 \tilde{w}}{d\tilde{x}^3} + \frac{d\tilde{T}_o}{d\tilde{x}} &= 0 \end{aligned} \right\} \quad \text{at } x = 0 \text{ and } x = 1, \quad (6.7)$$

and the pinned-pinned boundary conditions are

$$\left. \begin{aligned} \tilde{w} &= 0 \\ \frac{d^2 \tilde{w}}{d\tilde{x}^2} + \tilde{T}_o &= 0 \end{aligned} \right\} \quad \text{at } x = 0 \text{ and } x = 1, \quad (6.8)$$

As a test case to illustrate the difference in the solutions subjected to these types of boundary conditions, (6.5) was solved for a beam with gravity, see Fig. 6.2 with several levels for the firmness of the foundation. With the free boundary boundary conditions, the beam uniformly compresses the foundation and remains flat (sinking lower with the weaker spring constants). With pinned boundary conditions, where the ends of the beam are held at fixed positions, the beam deforms, but follows the same trend as expected, in the middle of the domain.

Two sets of pre-stressed beam shapes, flat vs. a deformed state,

$$\tilde{w}_{0a} = 0 \quad (\text{flat}), \quad \tilde{w}_{0b} = 0.01 \cos(2\pi\tilde{x}) \quad (\text{deformed}), \quad (6.9)$$

were considered to illustrate difference between flat plates and weakly curved shells subjected to two sets of imposed temperature fields,

$$\tilde{T}_{oa} = \gamma \quad (\text{uniform}), \quad \tilde{T}_{ob} = \gamma\tilde{x}^2 \quad (\text{quadratic growth}). \quad (6.10)$$

While the temperature distribution enters equation (6.5) as a second-derivative of \tilde{T}_o , the influence of the uniform temperature field does play a nontrivial role in determining the solution, not as internal stresses, but through its presence in the boundary conditions (6.7) or (6.8). See Fig. 6.3 for the thermally induced deflections of a flat beam. As expected, larger temperatures resulted in larger deflections. The symmetric nature of the uniform temperature distribution T_{oa} resulted in symmetric deformations, while the asymmetric nature of T_{ob} resulted in asymmetric deformations. The overall amplitude of the deflection for a given intensity of the temperature field appears independent of the boundary conditions (the only difference is a very translation). The deflections due to the non-uniform temperature distribution were smaller than for the corresponding uniform field, which is very plausible since $T_{oa}(x) \geq T_{ob}(x)$ with equality holding at $x = 1$ and $T_{oa}(0) = 0$ (hence stronger differences are expected at the left end of the beam). Fig. 6.4 shows corresponding results on an initially-deformed beam; in this case more intense thermal forcing was necessary in order to produce visible perturbations from the relatively large initial deformation \tilde{w}_0 .

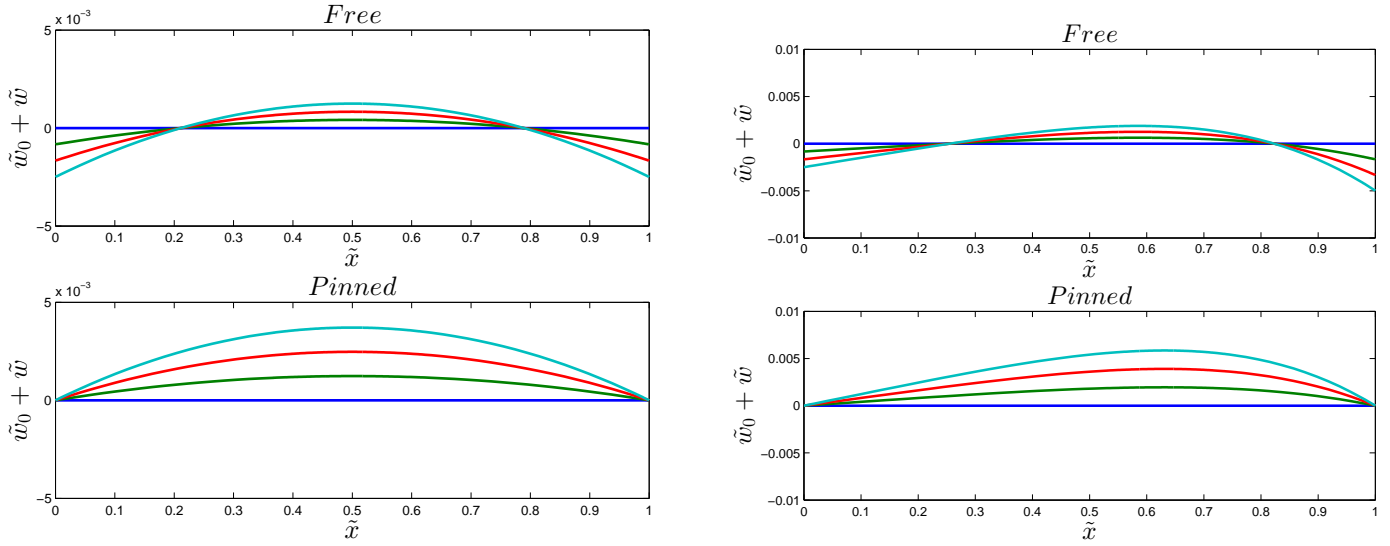


Figure 6.3: Deflections due to thermal stresses on a flat beam ($\tilde{w}_0 = 0$) with no other loading ($\tilde{P} = 0$) and a fixed foundation stiffness ($K = 1$): (Left) Uniform temperature field $\tilde{T}_o = \gamma$, (Right) Quadratic temperature field $\tilde{T}_o = \gamma\tilde{x}^2$, both with $\gamma = 0$ (blue), $\gamma = 0.01$ (green), $\gamma = 0.02$ (red), $\gamma = 0.03$ (cyan).

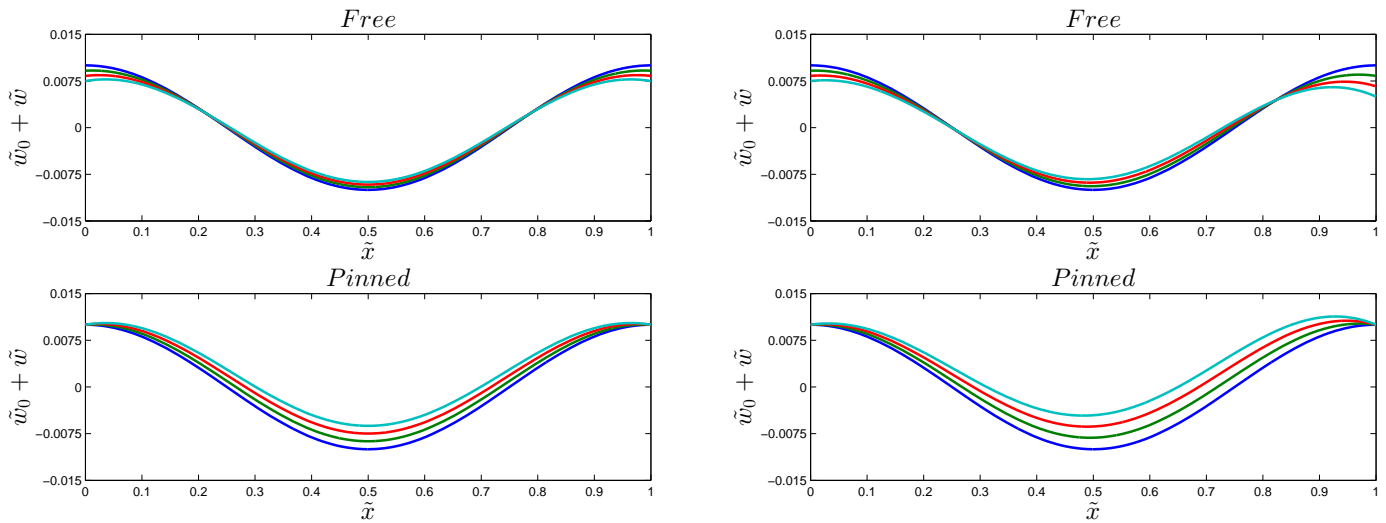


Figure 6.4: Deflections due to thermal stresses on an initially deformed beam ($\tilde{w}_0 = 0.01 \cos(2\pi\tilde{x})$) with no other loading ($\tilde{P} = 0$) and a fixed foundation stiffness ($K = 1$): (Left) Uniform temperature field $\tilde{T}_o = \gamma$, (Right) Quadratic temperature field $\tilde{T}_o = \gamma\tilde{x}^2$, both with $\gamma = 0$ (blue), $\gamma = 0.05$ (green), $\gamma = 0.10$ (red), $\gamma = 0.15$ (cyan).

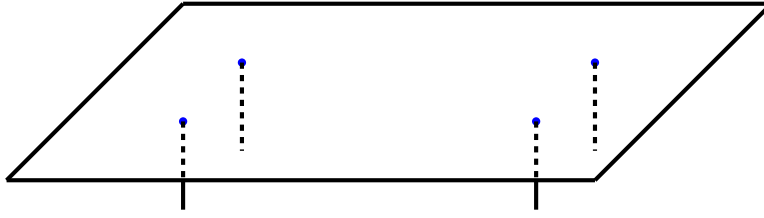


Figure 7.1: Schematic representation of a flat plate with free boundary conditions, supported by four interior pins.

7 Two-dimensional Numerical Simulations

As a step toward efficient direct numerical solution of the full two-dimensional system of governing equations, here we are interested in solving a biharmonic equation of the form¹⁵

$$D\nabla^4 w = f, \quad (7.1)$$

where the dependent variable $w(x, y)$ represents the deflection of a thin glass plate subject to a applied vertical forces, $f(x, y) = \sum_i F_i$. This Poisson-type (inhomogeneous forced) problem for the biharmonic operator does not exactly match either of the governing equations for the full shell problem, but it captures the fundamental nature of the numerical problems involved, taking the forms of fourth-order elliptic boundary value problems with biharmonic operators.

Examples of forces applied to the plate include gravity and pin supports (motivated by [1]). Figure 7.1 illustrates the problem setting for some of the example computations. We note that in order for an equilibrium solution to exist to (7.1), there must be no net force $\iint f \, dy \, dx = 0$ and no net torques.

We will illustrate how to solve equation (7.1) on an infinite domain using the thin-plate spline method and on a finite square domain $\Omega = [x_a, x_b] \times [y_a, y_b]$ using standard finite difference method of second order accuracy. For the finite domain case, one of following sets of boundary conditions will be considered:

$$w|_{\partial\Omega} = 0, \quad \left. \frac{\partial w}{\partial n} \right|_{\partial\Omega} = 0 \quad (\text{Clamped BCs}) \quad (7.2)$$

or

$$\left. \frac{\partial^2 w}{\partial n^2} + \nu \frac{\partial^2 w}{\partial s^2} \right|_{\partial\Omega} = 0, \quad \left. \frac{\partial}{\partial n} (\nabla^2 w) + (1 - \nu) \frac{\partial}{\partial s} \left(\frac{\partial^2 w}{\partial n \partial s} \right) \right|_{\partial\Omega} = 0 \quad (\text{Free BCs}) \quad (7.3)$$

where n is the coordinate in the outward normal direction and s is the coordinate along a straight segment of the boundary of the rectangular domain.

7.1 Thin-plate spline method: infinite domain

Thin-plate spline method is applied to solve the biharmonic equation with pin supports in infinite domain.¹⁶ From the balance between the forces from pin support, the gravity force and the in-plate strains, we have

$$m \frac{\partial^2 w}{\partial t^2} = -D\nabla^4 w + \bar{P} + \sum_i^N K_i \delta(X_i, Y_i). \quad (7.4)$$

For the steady state that we are interested in, the governing equations read

$$D\nabla^4 w = \bar{P} + \sum_{i=1}^N K_i \delta(X_i, Y_i). \quad (7.5a)$$

$$w(X_i, Y_i) = w_i, \quad \text{for } i = 1, \dots, N, \quad (7.5b)$$

where (7.5b) describes the position and height of a set of N pins.

To solve the equation (7.5) we set $w = \bar{w} + w_0$, where \bar{w} solves

$$D\nabla^4 \bar{w} = \sum_{i=1}^N K_i \delta(X_i, Y_i), \quad (7.6)$$

¹⁵This section is from work by Valeria Barra, Hangjie Ji and Longfei Li

¹⁶This sub-section from material by Hangjie Ji and Bob Ronkese

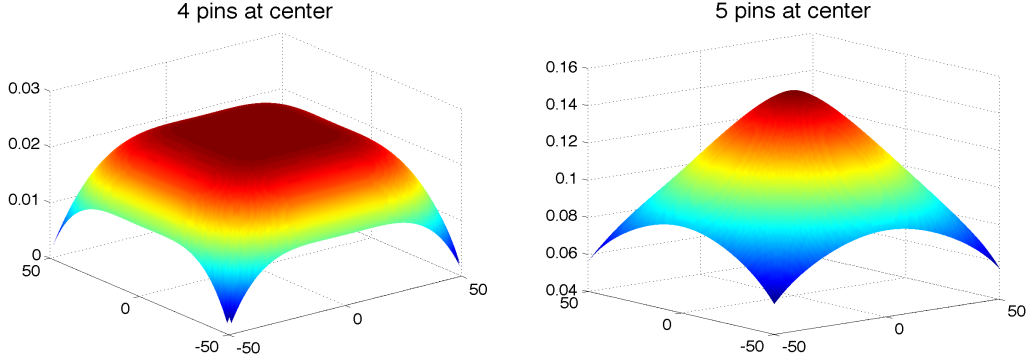


Figure 7.2: Thin-plate splines interpolation with four (left) and five (right) pins placed near the center of the domain.

where w_0 solves

$$D\nabla^4 w_0 = \bar{P} \quad (7.7)$$

and \bar{w} is also a minimizer of the bending energy

$$I(w) = \iint_{\Omega} \{(w_{xx})^2 + 2(w_{xy})^2 + (w_{yy})^2\} dx dy. \quad (7.8)$$

Using the fundamental solution of the biharmonic equation, the interpolating function of thin-plate splines that solve (7.6) takes the form

$$\bar{w}(x, y) = A + Bx + Cy + \sum_{i=1}^N K_i r_i^2 \ln r_i, \quad (7.9)$$

where $r_i = (x - X_i)^2 + (y - Y_i)^2$. The balance between the gravity and point-source forces from pins requires that

$$\sum_{i=1}^N K_i = -\bar{P}. \quad (7.10)$$

For symmetrically placed pins, two more constraints

$$\sum_{i=1}^N K_i X_i = 0, \quad \sum_{i=1}^N K_i Y_i = 0, \quad (7.11)$$

give conditions to ensure the plate has no net rotational moments, which determine all the coefficients in the interpolating function (7.9). Since w_0 is a particular solution to (7.5), with $K_i = 0$ for all $i = 1, \dots, N$, we set

$$w_0 = \frac{P}{24} (\alpha(x^4 + y^4) + 6(1 - 2\alpha)x^2y^2). \quad (7.12)$$

Therefore a general solution to (7.5) is

$$w(x, y) = A + Bx + Cy + \sum_{i=1}^N K_i r_i^2 \log r_i + \frac{P}{24} (\alpha(x^4 + y^4) + 6(1 - 2\alpha)x^2y^2). \quad (7.13)$$

Numerical results with thin-plate splines for infinite domain solution with different number of pins are shown in Figure 7.2. In the left plot of Figure 7.2, there are four pins of equal height supporting the glass sheet, while in the right, there are 5 supporting pins with the center one positioning higher than the rest four pins.

As a simple example, we show the explicit calculation for the determination of the coefficients $\{a, b_1, b_2, K_i\}$ for a problem with four pins and $\bar{P} = 0$. Let

$$\begin{aligned} (x_1, y_1) &= (1, 1), & (x_2, y_2) &= (-1, 1), & (x_3, y_3) &= (-1, -1), & (x_4, y_4) &= (1, -1), \\ w(1, 1) &= W_1, & w(-1, 1) &= W_2, & w(-1, -1) &= W_3, & w(1, -1) &= W_4. \end{aligned}$$

Substituting into the equation for $w(x, y)$ yields the system of equations,

$$\begin{aligned} W_1 &= A + B + C + (20 \ln 2)K_1, & W_2 &= A - B + C + (20 \ln 2)K_2, \\ W_3 &= A - B - C + (20 \ln 2)K_3, & W_4 &= A + B - C + (20 \ln 2)K_4. \end{aligned}$$

This is a system of four equations for seven unknowns ($A, B, C, K_1, K_2, K_3, K_4$). The equations on the net forces and moments, (7.10) with $\bar{P} = 0$ and (7.11), complete the system,

$$K_1 + K_2 + K_3 + K_4 = 0, \quad K_1 - K_2 - K_3 + K_4 = 0, \quad K_1 + K_2 - K_3 - K_4 = 0.$$

Solving this system of 7 linear equations using `Mathematica` yields

$$\begin{aligned} A &= \frac{1}{4}(W_1 + W_2 + W_3 + W_4), & B &= \frac{1}{4}(W_1 - W_2 - W_3 + W_4), & C &= \frac{1}{4}(W_1 + W_2 - W_3 - W_4), \\ K_1 &= \frac{W_1 - W_2 + W_3 - W_4}{80 \ln 2}, & K_2 &= -K_1, & K_3 &= K_1, & K_4 &= -K_1. \end{aligned}$$

For problems involving plates with free boundary conditions and forces localized to a region far from any boundaries, the thin-plate spline representation of the solution (7.13) can give a good estimate of the deflection in a small central region. We now turn to the numerical problem of solving for finite-sized plates, which intrinsically requires the application of boundary conditions.

7.2 Standard Finite Difference Method: finite domain

To solve the biharmonic equation (7.1) subject to either the clamped edge or free edge boundary conditions on a finite square domain ($\Omega = [x_a, x_b] \times [y_a, y_b]$), we use the standard second order centered finite difference method. The domain is discretized using a Cartesian grid Ω_h with grid spacing given by we discretize the domain with grid points defined as:

$$\begin{cases} x_i &= x_a + i\Delta x, & i &= 0, 1, 2, \dots, N \\ y_j &= y_a + j\Delta y, & j &= 0, 1, 2, \dots, M \end{cases} \quad (7.14)$$

$x_a \equiv x_0, y_a \equiv y_0, x_b = x_N, y_b = y_M$, and where $\Delta x = (x_b - x_a)/(N - 1)$, $\Delta y = (y_b - y_a)/(M - 1)$, where N and M are the number of grid points along x - and y -axes, respectively.

The second-order accurate, centered finite difference approximation of w_{xx} and w_{yy} at point (x_i, y_i) are given by

$$w_{xx}(x_i, y_j) \approx \frac{W_{i+1,j} - 2W_{ij} + W_{i-1,j}}{\Delta x^2}, \quad w_{yy}(x_i, y_j) \approx \frac{W_{i,j+1} - 2W_{ij} + W_{i,j-1}}{\Delta y^2},$$

where W_{ij} is the numerical approximation of $w(x_i, y_j)$. We vectorize the discrete solutions $\{W_{ij}\}$ in the following way,

$$W = \begin{pmatrix} W_{1,1} \\ W_{1,2} \\ \vdots \\ W_{1,M} \\ \vdots \\ W_{N,1} \\ W_{N,2} \\ \vdots \\ W_{N,M} \end{pmatrix}, \quad (7.15)$$

and introduce the a $n \times n$ matrix D_n^2

$$D_n^2 = \begin{pmatrix} -2 & 1 & & \dots & 0 & 0 & 0 \\ 1 & -2 & 1 & & & \dots & 0 & 0 \\ 0 & 1 & -2 & 1 & & & \dots & 0 \\ \vdots & & & \ddots & \ddots & \ddots & & \vdots \\ 0 & \dots & 0 & 1 & -2 & 1 & & 0 \\ 0 & 0 & \dots & & 1 & -2 & 1 & \\ 0 & 0 & 0 & \dots & & 1 & -2 & \end{pmatrix}_{n \times n}. \quad (7.16)$$

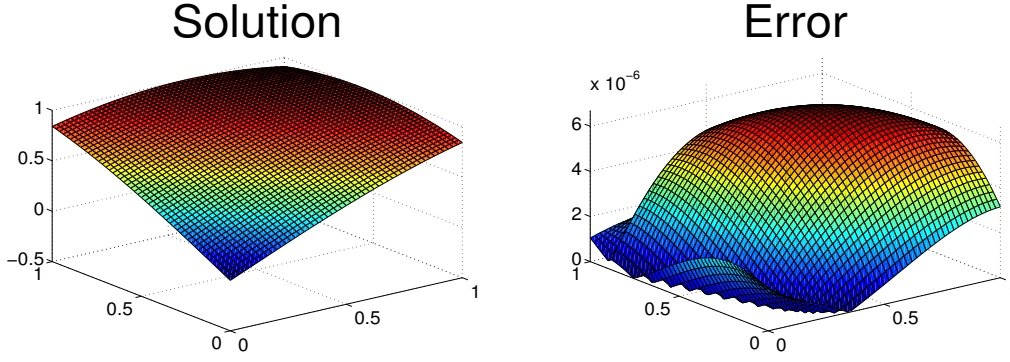


Figure 7.3: Test problem for the forced biharmonic equation, with solution (7.22) subject to free-edge boundary conditions (left) and the computational error, $w - w_e$ (right).

Noting that $\nabla^4 w = w_{xxxx} + 2w_{xxyy} + w_{yyyy}$, we then can construct the differentiation matrix \mathcal{D}_{∇^4} for the biharmonic operator ∇^4 as,

$$\mathcal{D}_{\nabla^4} = \mathcal{D}_{xx}\mathcal{D}_{xx} + 2\mathcal{D}_{xx}\mathcal{D}_{yy} + \mathcal{D}_{yy}\mathcal{D}_{yy}, \quad (7.17)$$

where

$$\mathcal{D}_{xx} = \frac{1}{\Delta x^2} D_N^2 \otimes I_M, \quad \mathcal{D}_{yy} = \frac{1}{\Delta y^2} I_N \otimes D_M^2. \quad (7.18)$$

Here \otimes represents the Kronecker product, and I_n is an $n \times n$ identity matrix. Therefore, the discretized approximation of equation (7.1) can be written as a system of linear equations

$$D \mathcal{D}_{\nabla^4} W = F. \quad (7.19)$$

Here F is the vectorized version of the discrete forces $\{f_{ij}\}$. Equation (7.19) can be easily solved with the backslash operator in MATLAB.

7.2.1 Implementation of Boundary Conditions

To implement the first set of boundary conditions (7.2), we need to specify homogeneous Dirichlet and Neumann boundary conditions at the four edges of the rectangular domain. Call them $L : x = x_a, y_a < y < y_b$, $B : x_a < x < x_b, y = y_a$, $R : x = x_b, y_a < y < y_b$, $T : x_a < x < x_b, y = y_b$ (for left, bottom, right and top edges respectively). Therefore we use:

$$w = 0, \quad \text{for } x_{i,j} \text{ on } L, B, R, T \quad (7.20a)$$

$$\frac{\partial w}{\partial n} = 0 \quad \text{for } x_{i,j} \text{ on } L, B, R, T \quad (7.20b)$$

To implement (7.20b), we identify the directional derivative for the outward normal to the domain, on L : $\frac{\partial}{\partial n} = -\frac{\partial}{\partial x}$, on B : $\frac{\partial}{\partial n} = -\frac{\partial}{\partial y}$, on R : $\frac{\partial}{\partial n} = \frac{\partial}{\partial x}$, and on T : $\frac{\partial}{\partial n} = \frac{\partial}{\partial y}$.

Subsequently, the second set of boundary conditions (7.3) can be expressed as

$$w_{xx} + \nu w_{yy} = 0 \quad \text{for } x_{i,j} \text{ on } L, R \quad (7.21a)$$

$$w_{yy} + \nu w_{xx} = 0 \quad \text{for } x_{i,j} \text{ on } T, B \quad (7.21b)$$

$$w_{xxx} + (2 - \nu)w_{xyy} = 0 \quad \text{for } x_{i,j} \text{ on } L, R \quad (7.21c)$$

$$w_{yyy} + (2 - \nu)w_{xxy} = 0 \quad \text{for } x_{i,j} \text{ on } T, B \quad (7.21d)$$

7.2.2 Test Problem

We first formulate a test problem using the method of manufactured solution to validate the biharmonic solver. The forcing f is specified so that a chosen function becomes an exact solution to the biharmonic equation (7.1). To be specific, we chose the exact solution to be

$$w_e = \sin(x + y), \quad (7.22)$$

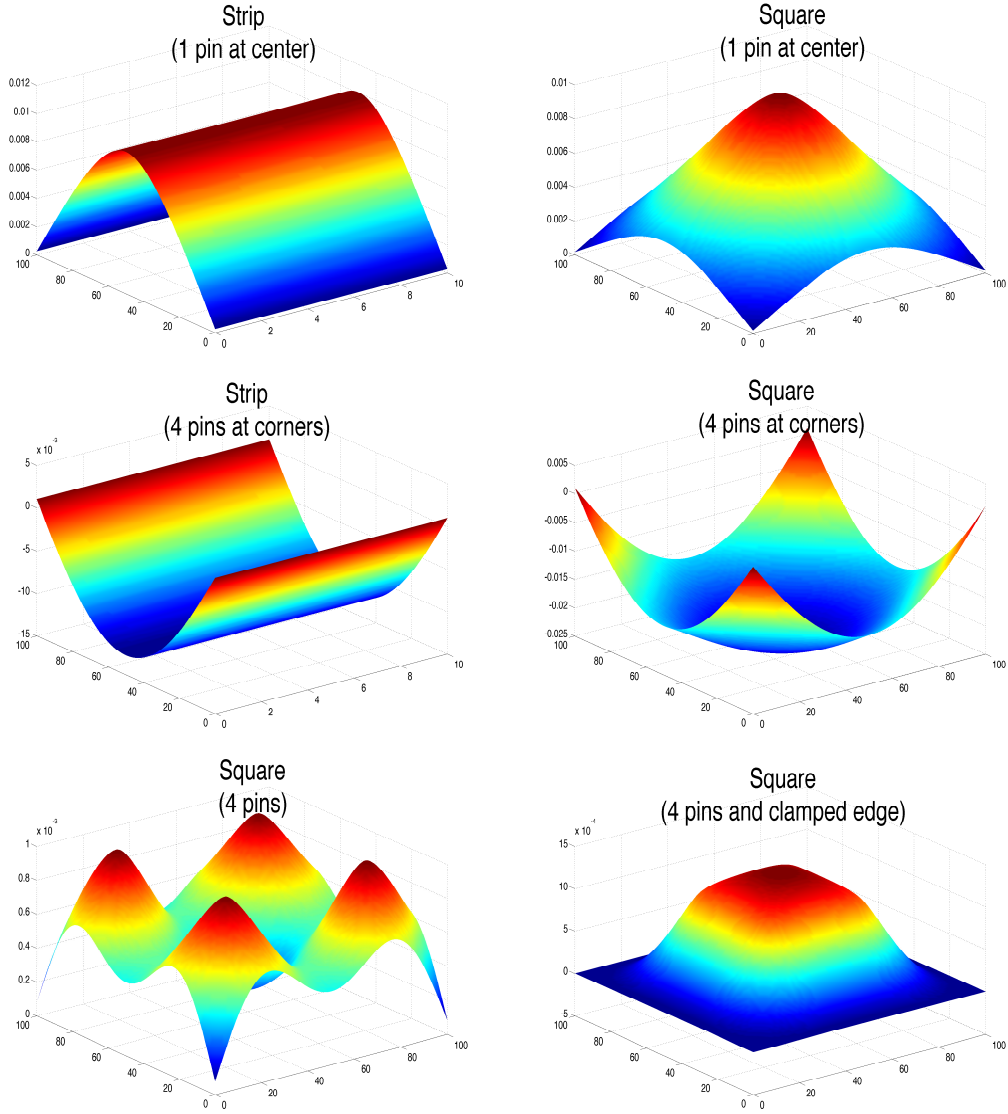


Figure 7.4: Numerical simulations for solution of the biharmonic equation with various configurations (all with free-edge boundary conditions except the final plot).

and the forcing $f(x, y)$ is specified by $f_e \equiv D\nabla^4 w_e$. We numerically solve the equation

$$D\nabla^4 w = f_e$$

using the biharmonic solver, and compare the numerical results W with the exact solution w_e , see Figure 7.3.

7.2.3 Numerical Simulations

Figure 7.4 shows results with various settings for boundary conditions and pin supports. At each pin, a value for the deflection as imposed as a point-wise Dirichlet condition on w . Physically based parameters are used here ($D = 10^5$ and $\nu = 0.22$). Note that free edge boundary conditions are imposed for all the plots in Figure 7.4 except the last one, which is solved with clamped edge boundary conditions.

7.3 Approaches to solving the nonlinear system

The full model is a system of two nonlinear equations for w and ϕ of the following form

$$-\frac{1}{Eh}\nabla^4\varphi = \left(\frac{\partial^2 w_0}{\partial x^2}\frac{\partial^2 w}{\partial y^2} - 2\frac{\partial^2 w_0}{\partial x\partial y}\frac{\partial^2 w}{\partial x\partial y} + \frac{\partial^2 w_0}{\partial y^2}\frac{\partial^2 w}{\partial x^2}\right) + \left(\frac{\partial^2 w}{\partial x^2}\frac{\partial^2 w}{\partial y^2} - \left(\frac{\partial^2 w}{\partial x\partial y}\right)^2\right) + \nabla^2(\alpha T) \quad (7.23a)$$

$$D\nabla^4 w = \left(\frac{\partial^2 w_0}{\partial x^2} \frac{\partial^2 \varphi}{\partial y^2} - 2 \frac{\partial^2 w_0}{\partial x \partial y} \frac{\partial^2 \varphi}{\partial x \partial y} + \frac{\partial^2 w_0}{\partial y^2} \frac{\partial^2 \varphi}{\partial x^2} \right) + \left(\frac{\partial^2 w}{\partial x^2} \frac{\partial^2 \varphi}{\partial y^2} - 2 \frac{\partial^2 w}{\partial x \partial y} \frac{\partial^2 \varphi}{\partial x \partial y} + \frac{\partial^2 w}{\partial y^2} \frac{\partial^2 \varphi}{\partial x^2} \right) + P_{\text{ext}} \quad (7.23b)$$

where w_0 and T are given. The system can be symbolically written as

$$\begin{cases} \nabla^4 \varphi = -\frac{1}{2} Eh \mathcal{L} w + \mathcal{N}_1(w) + d(T), \\ D\nabla^4 w = \mathcal{L} \varphi + \mathcal{N}_2(\varphi, w) + P_{\text{ext}}. \end{cases} \quad (7.24)$$

Here $d(T) = -Eh\nabla^2(\alpha T)$, \mathcal{N}_1 and \mathcal{N}_2 are the nonlinear terms and \mathcal{L} is a linear operator given by

$$\mathcal{L} = \left(\frac{\partial^2 w_0}{\partial x^2} \frac{\partial^2}{\partial y^2} - 2 \frac{\partial^2 w_0}{\partial x \partial y} \frac{\partial^2}{\partial x \partial y} + \frac{\partial^2 w_0}{\partial y^2} \frac{\partial^2}{\partial x^2} \right).$$

7.3.1 Linear case

To begin with, we may consider dropping the nonlinear terms and solving a simplified system

$$\begin{cases} \nabla^4 \varphi = -\frac{1}{2} Eh \mathcal{L} w + d(T), \\ D\nabla^4 w = \mathcal{L} \varphi + P_{\text{ext}}. \end{cases} \quad (7.25)$$

1. Direct solver: we can discretize the system using finite difference method. Let's denote \mathcal{D}_{∇^4} and \mathcal{D}_L the differentiation matrices of the operators ∇^4 and \mathcal{L} , respectively. $\Phi = \{\varphi_{ij}\}$ and $W = \{w_{ij}\}$ represents vectors of solutions at all the grid points. Then, the system (7.25) becomes a system of linear equations:

$$\begin{pmatrix} \mathcal{D}_{\nabla^4} & \frac{1}{2} Eh \mathcal{D}_L \\ -\mathcal{D}_L & DD_{\nabla^4} \end{pmatrix} \begin{pmatrix} \Phi \\ W \end{pmatrix} = \begin{pmatrix} \mathbf{d}(\mathbf{T}) \\ \mathbf{p} \end{pmatrix}. \quad (7.26)$$

We can use the MATLAB backslash command or some other methods to directly solve (7.26).

- Pro's: Implementation in MATLAB is straightforward.
 - Con's: the system we need to solve becomes double in size (resolution becomes limited by available computer memory); this method is not extensible to nonlinear case.
2. Iterative solver: we can iteratively solve the system (7.25) with $\{\varphi^n, w^n\}$ converging to the solution as n increases. We solve two biharmonic equations separately at each iteration step,

$$\begin{cases} \nabla^4 \varphi^{n+1} = -\frac{1}{2} Eh \mathcal{L} w^n + d(T), \\ D\nabla^4 w^{n+1} = \mathcal{L} \varphi^{n+1} + P_{\text{ext}}. \end{cases} \quad (7.27)$$

At the time we solve the equation for φ^{n+1} , the right-hand-side of the biharmonic equation is known. We therefore just need a biharmonic solver to solve

$$\nabla^4 \varphi^{n+1} = f(w^n), \text{ where } f(w^n) \text{ is known.} \quad (7.28)$$

When φ^{n+1} is solved, the right-hand-side of the w equation becomes known. We can use the biharmonic solver again to solve for w^{n+1} :

$$D\nabla^4 w^{n+1} = g(\varphi^{n+1}), \text{ where } g(\varphi^{n+1}) \text{ is known.} \quad (7.29)$$

- Pro's: We can reuse the biharmonic solver that has been developed; the size of the equations we need to solve does not increase; we can easily extend this method to the full nonlinear equation (7.24).
- Cons': We are not sure about the convergence rate of the iteration, or if it converges at all.
- Possible ways to prove or disprove convergence of the iteration:
 - (a) We Fourier transform the system (7.27). We prove the iteration converges for Fourier mode.
 - (b) We discretize the system using finite difference method. Then, we end up with

$$\begin{cases} \mathcal{D}_{\nabla^4} \Phi^{n+1} = -\frac{1}{2} Eh \mathcal{D}_L W^n + d(T), \\ DD_{\nabla^4} W^{n+1} = \mathcal{D}_L \Phi^{n+1} + P_{\text{ext}}. \end{cases} \quad (7.30)$$

or equivalently,

$$\begin{pmatrix} \mathcal{D}_{\nabla^4} & \mathbf{0} \\ -\mathcal{D}_L & DD_{\nabla^4} \end{pmatrix} \begin{pmatrix} \Phi^{n+1} \\ W^{n+1} \end{pmatrix} = \begin{pmatrix} \mathbf{0} & -\frac{1}{2}Eh\mathcal{D}_L \\ \mathbf{0} & \mathbf{0} \end{pmatrix} \begin{pmatrix} \Phi^n \\ W^n \end{pmatrix} + \begin{pmatrix} \mathbf{d}(\mathbf{T}) \\ \mathbf{p} \end{pmatrix} \quad (7.31)$$

We define the residual to be

$$\mathbf{R}^{n+1} = \begin{pmatrix} \Phi^{n+1} - \Phi^n \\ W^{n+1} - W^n \end{pmatrix}. \quad (7.32)$$

Equation (7.30) implies

$$\begin{pmatrix} \mathcal{D}_{\nabla^4} & \mathbf{0} \\ -\mathcal{D}_L & DD_{\nabla^4} \end{pmatrix} \mathbf{R}^{n+1} = \begin{pmatrix} \mathbf{0} & -\frac{1}{2}Eh\mathcal{D}_L \\ \mathbf{0} & \mathbf{0} \end{pmatrix} \mathbf{R}^n. \quad (7.33)$$

Let

$$A = \begin{pmatrix} \mathcal{D}_{\nabla^4} & \mathbf{0} \\ -\mathcal{D}_L & DD_{\nabla^4} \end{pmatrix} \quad B = \begin{pmatrix} \mathbf{0} & -\frac{1}{2}Eh\mathcal{D}_L \\ \mathbf{0} & \mathbf{0} \end{pmatrix}, \quad (7.34)$$

then we have

$$\mathbf{R}^{n+1} = A^{-1}B\mathbf{R}^n. \quad (7.35)$$

If we can show $\|A^{-1}B\| < 1$, then the iteration scheme for the discretized system (7.30) is convergent.

7.3.2 Nonlinear case

1. Monolithic solver: we can solve the whole system(7.24) using Newton's method. To be specific, we discretize the system using finite difference method:

$$\begin{pmatrix} \mathcal{D}_{\nabla^4} & \frac{1}{2}Eh\mathcal{D}_L \\ -\mathcal{D}_L & DD_{\nabla^4} \end{pmatrix} \begin{pmatrix} \Phi \\ W \end{pmatrix} = \begin{pmatrix} \mathbf{d}(\mathbf{T}) \\ \mathbf{p} \end{pmatrix} + \begin{pmatrix} \mathcal{N}_1(\mathbf{W}) \\ \mathcal{N}_2(\Phi, \mathbf{W}) \end{pmatrix}. \quad (7.36)$$

Define

$$\mathbf{F}(\Phi, W) = \begin{pmatrix} \mathcal{D}_{\nabla^4} & \frac{1}{2}Eh\mathcal{D}_L \\ -\mathcal{D}_L & DD_{\nabla^4} \end{pmatrix} \begin{pmatrix} \Phi \\ W \end{pmatrix} - \begin{pmatrix} \mathcal{N}_1(\mathbf{W}) \\ \mathcal{N}_2(\Phi, \mathbf{W}) \end{pmatrix} - \begin{pmatrix} \mathbf{d}(\mathbf{T}) \\ \mathbf{p} \end{pmatrix}. \quad (7.37)$$

We can use Newton's method to find the zeros of \mathbf{F} . Let's denote

$$\begin{pmatrix} \Phi \\ W \end{pmatrix} = \mathbf{U}.$$

To solve $\mathbf{F}(\mathbf{U}) = \mathbf{0}$ using Newton's method:

$$\mathbf{U}^{n+1} = \mathbf{U}^n - (J_{\mathbf{F}}(\mathbf{U}^n))^{-1} \mathbf{F}(\mathbf{U}^n),$$

where $J_{\mathbf{F}}(\mathbf{U}^n)$ is the Jacobian matrix of \mathbf{F} evaluated at \mathbf{U}^n .

- Pro's: the method is straight forward
- Con's: Implementation is hard, especially evaluating the Jacobian matrix. The system size is doubled which is computationally more expensive.

2. Iterative solver: we solve the system (7.24) by iteration. One possible formulation for iteration is

$$\begin{cases} \nabla^4 \varphi^{n+1} = -\frac{1}{2}Eh\mathcal{L}w^n + \mathcal{N}_1(w^n) + d(T), \\ D\nabla^4 w^{n+1} = \mathcal{L}\varphi^{n+1} + \mathcal{N}_2(\varphi^n, w^n) + P_{\text{ext}}. \end{cases} \quad (7.38)$$

- Pro's: easy to implement in MATLAB; we can reuse our biharmonic solver; system size does not increase.
- Con's: we are not sure if the formulation (7.38) will converge. We might need formulate some other iteration scheme, for example, treating the nonlinear terms semi-implicitly.

8 Directions for further work: inverse problems

The work outlined here that was accomplished during the workshop covered several aspects of the formulation and computation of the direct problem governing the state of a steady weakly curved thin shell (and the 1-D analogue for a beam). This is necessary background for approaching the inverse problems described in the introduction on backing out the precast deflection and/or thermal stresses given the overall deflection.

Computational methods for inverse problems in general, and in thermoelasticity in particular [11] may require regularization of an ill-posed or ill-conditioned system of equations and iterative solution in terms of an optimization problem. Here we very briefly outline an approach¹⁷ that could be applied to solving the inverse problem for determining the precast deflection w_0 from observed data $f_{\text{obs}}(x, y)$ on the full deflection f ($f = w + w_0$) if we are given the induced deflection w . Expressing the system in the form (7.37), we assume some initial guess for w_0 , call it w_0^0 and that we can apply the earlier computational methods to solve the problem

$$\mathbf{F}(\mathbf{U}; \mathbf{W}_0^n) = \begin{pmatrix} 0 \\ \mathbf{v}^n \end{pmatrix} \quad (8.1)$$

where the function $v(x, y)$ is taken so as to minimize the regularized functional

$$\min_{v, w_0} J(v, w_0) \quad \text{where} \quad J(v, w_0) \equiv \alpha \|v\|^2 + \|f_{\text{obs}} - (w + w_0)\|^2 \quad (8.2)$$

for some $\alpha > 0$. Expressed in this form, this optimization problem can be solved iteratively starting from an initial guess for $v = v^0$ using methods from numerical linear algebra such as conjugate gradient approaches [12, Chap. 10].

References

- [1] J.S. Abbott, D.R. Harvey, and C.R. Ustanik. Methods and apparatus for estimating gravity-free shapes, 2015. US Patent 9,031,813.
- [2] M. Batista. New analytical solution for bending problem of uniformly loaded rectangular plate supported on corner points. *The IES Journal Part A: Civil & Structural Engineering*, 3(2):75–84, 2010.
- [3] M. Batista. Uniformly loaded rectangular thin plates with symmetrical boundary conditions. *arXiv preprint arXiv:1001.3016*, 2010.
- [4] B. A. Boley and J. H. Weiner. *Theory of thermal stresses*. Dover publications, 2012.
- [5] M. R. Eslami, R. B. Hetnarski, J. Ignaczak, N. Noda, N. Sumi, and Y. Tanigawa. *Theory of elasticity and thermal stresses*. Springer, 2013.
- [6] W. Flügge. *Stresses in shells*. Springer, 2013.
- [7] B. Häggblad and K.-J. Bathe. Specifications of boundary conditions for Reissner/Mindlin plate bending finite elements. *International Journal for Numerical Methods in Engineering*, 30(5):981–1011, 1990.
- [8] P. Howell, G. Kozyreff, and J. Ockendon. *Applied solid mechanics*. Cambridge University Press, 2009.
- [9] D. Krause and H. Loch. *Mathematical simulation in glass technology*. Springer Science & Business Media, 2012.
- [10] L. D. Landau and E. M. Lifshitz. *Elasticity theory*. Pergamon Press, 1975.
- [11] L. Marin, A. Karageorghis, and D. Lesnic. A numerical study of the SVD-MFS solution of inverse boundary value problems in two-dimensional steady-state linear thermoelasticity. *Numerical Methods for Partial Differential Equations*, 31(1):168–201, 2015.
- [12] W. H. Press, S. A. Teukolsky, W. T. Vetterling, and B. P. Flannery. *Numerical recipes 3rd edition: The art of scientific computing*. Cambridge university press, 2007.
- [13] R. Szilard. *Theories and applications of plate analysis: classical numerical and engineering methods*. John Wiley & Sons, 2004.

¹⁷From work by Pavel Dubovski

- [14] T. Tauchert. Thermal stresses in plates-statical problems. *Thermal stresses I*, 1:23–141, 1986.
- [15] T. R. Tauchert. Thermally induced flexure, buckling, and vibration of plates. *Applied Mechanics Reviews*, 44(8):347–360, 1991.
- [16] E. A. Thornton. Thermal buckling of plates and shells. *Applied Mechanics Reviews*, 46(10):485–506, 1993.
- [17] A. S. Usmani, J. M. Rotter, S. Lamont, A. M. Sanad, and M. Gillie. Fundamental principles of structural behaviour under thermal effects. *Fire Safety Journal*, 36(8):721–744, 2001.
- [18] M. A. Vaz, J. C. R. Cyrino, and V. E. Lourenço. Thermal buckling of beams on elastic foundation. In *Encyclopedia of Thermal Stresses*, pages 4884–4897. Springer, 2014.
- [19] E. Ventsel and T. Krauthammer. *Thin plates and shells: theory: analysis, and applications*. CRC press, 2001.
- [20] R. Wong. *Asymptotic approximations of integrals*, volume 34. SIAM, 2001.